# Product Validation and Inter-comparison Report (PVIR)
# Phase 2 Year 3

glaciers cci

| | |
|---|---|
| Prepared by: | Glaciers_cci consortium |
| Contract: | 4000109873/14/I-NB |
| Name: | Glaciers_cci-D4.1_PVIR |
| Version: | 1.6 |
| Date: | 21.12.2017 |

Contact:
Frank Paul
Department of Geography
University of Zurich
frank.paul@geo.uzh.ch

Technical Officer:
Stephen Plummer
ESA / ESRIN

UNIVERSITY OF OSLO

University of Zurich UZH

UNIVERSITY OF LEEDS

GAMMA REMOTE SENSING

enveo

# Document status sheet

| Version | Date | Changes | Approval |
|---|---|---|---|
| 0.1 | 22.05. 2013 | Initial draft | |
| 0.2 | 11.11. 2013 | extended ToC | |
| 0.3 | 24.01. 2014 | All sections completed apart from altimetry and area | |
| 0.4 | 02.02. 2014 | Altimetry and area added | |
| 0.5 | 25.03. 2014 | Minor edits from Technical Officer considered | |
| 0.6 | 02.05. 2014 | Revised according to comments of ESA | |
| 0.7 | 12.05. 2014 | Final check and editing | F. Paul |
| 0.8 | 31.05. 2014 | Final comments from Technical Officer integrated | |
| 0.9 | 16.06. 2014 | Final consortium feedback integrated | |
| 1.0 | 08.04. 2015 | New version for Phase 2 | T. Nagler |
| 1.1 | 29.06. 2015 | First consortium feedback integrated | |
| 1.2 | 31.07. 2015 | Edited version for submission | F. Paul |
| 1.3 | 27.04. 2016 | updated for input | |
| 1.4 | 21.07. 2016 | Year 2 update included | |
| 1.5 | 26.09. 2016 | Revised according to comments of ESA | |
| 1.5 | 26.11. 2016 | Small edits integrated. | |
| 1.6 | 18.10. 2017 | Year 3 update included | J. Wuite |
| 1.6 | 21.12.2017 | Comments from technical officer integrated | |

The work described in this report was done under ESA contract 4000109873/14/I-NB. Responsibility for the contents resides with the authors that prepared it.

Author team:
Thomas Nagler, Jan Wuite, Gabriele Bippus (all at Enveo), Frank Paul, Philipp Rastner (all at GIUZ), Robert McNabb, Christopher Nuth, Andreas Kääb (all at GUIO), Andrew Shepherd, Kate Briggs, Lin Gilbert (all at SEEL), Tazio Strozzi, Andreas Wiesmann (all at Gamma)

Glaciers_cci Technical Officer at ESA:
Stephen Plummer

Contract: 4000109873/14/I-NB
Product Validation and Inter-comparison Report (PVIR)

Name: Glaciers_cci-D4.1_PVIR
Version: 1.6
Date: 21.12. 2017
Page: 3

# Table of Contents

# 1. Introduction

## 1.1. Purpose

The Product Validation and Intercomparison Report (PVIR) provides a summary on the assessment of the quality and uncertainty of the products in the Climate Research Data Package that are made available to the public. Well-defined rules are specified to enable a standardized procedure for assessing the quality and uncertainty of the products for the various parameters.

## 1.2. Outline

The report is organized in 6 chapters:

- Chapter 1 is the overview and outline of the report.
- Chapter 2 and its subsections describe the methods and approaches for quality and uncertainty estimation of the products for glacier outlines (section 2.1), surface elevation change from DEM differencing (section 2.2) and altimetry (section 2.3) and ice velocity (section 2.4).
- Chapters 3 to 6 present the results of the quality assessment for the various products:
    - Chapter 3 describes the quality assessment for glacier outline products according to the methods described in section 2.1.
    - Chapter 4 describes the intercomparison and validation of elevation change products from DEM differencing as presented in section 2.2.
    - Chapter 5 describes the intercomparison and validation of elevation change products from altimetry following methods in section 2.3
    - Chapter 6 presents the validation, intercomparison and quality assessment of velocity products from SAR and optical satellite data using the methods and rules described in section 2.4.

Contract: 4000109873/14/I-NB
Product Validation and Inter-comparison Report (PVIR)

Name: Glaciers_cci-D4.1_PVIR
Version: 1.6
Date: 21.12. 2017
Page: 5

# 2. Methods for Quality Assessment

This section provides an overview on the methods for assessment of the quality of the glacier products. The section is organized according to the parameters glacier outlines, elevation change from DEM differencing and altimetry and ice velocity, and also identifies the main sources of errors in the retrieval of the products.

## 2.1. Glacier Outlines

### 2.1.1. Methods for validation

Strict validation of glacier outlines is difficult for both practical and theoretical reasons. On the one hand, suitable validation datasets (e.g. acquired in the same week from a higher-resolution sensor) are seldom available, on the other hand the definition of what belongs to a glacier is not unique among different analysts and differences in glacier outlines might express the variability of interpretation rather than a quality issue (cf. Section 3.1 in UCRv2). For these reasons, a comparison with reference datasets can only provide an estimate of accuracy rather than error. Another point to consider is that the outlines are not a pure algorithm product, but are already manually corrected and adjusted against the remote sensing data used or other datasets (e.g. corrections are required for debris cover, seasonal snow or shadow). It is important to note that the testing of the impact of different algorithms or thresholds on product quality is not reported here. Methods to determine accuracy or uncertainty vary with the available datasets and the effort of the analyst. A short summary of the methods for quality assessment of glacier outlines is given in Table 2.1, summarizing key characteristics of the test. Further specifications of the individual quality assessment tests are given in the following subsections.

| Test | Comparison | Calculation | Statistics | Measure | Metrics | Unit |
|---|---|---|---|---|---|---|
| QA-GO-1 | Glacier outline position vs field data | point by point | mean, STD | absolute | scalar | m |
| QA-GO-2 | Distance of outlines | variability along line | mean, STD | absolute | scalar | m |
| QA-GO-3 | Overlay of outlines | visual interpretation | differences | qualitative | text | - |
| QA-GO-4 | Area variability | total size per glacier | mean, STD | relative | scalar | % ($km^2$) |
| QA-GO-5 | Area differences | omission/commission | sums | absolute | scalar | % ($km^2$) |
| QA-GO-6 | Multiple independent digitizing of outlines | variability | mean, STD | relative | scalar | % ($km^2$) |
| QA-GO-7 | Buffer (area diff.) | add ½ or 1 pixel | range | relative | scalar | % |

*Table 2.1: Overview of the different possibilities to assess product accuracy for glacier area. STD is standard deviation, diff. is difference.*

### 2.1.2. QA-GO-1: Outline position

If DGPS data of the terminus position (or other glacier parts) from the field are available, these can be directly compared to those derived from remote sensing data. A good temporal coincidence is mandatory, in particular in regions with rapid glacier changes.

Contract: 4000109873/14/I-NB

**Product Validation and Inter-comparison Report (PVIR)**

Name: Glaciers_cci-D4.1_PVIR
Version: 1.6
Date: 21.12. 2017
Page: 6

### 2.1.3. QA-GO-2: Outline distance

If high-quality outlines from other (independent) sources are available, their positional difference can be measured for individual glaciers with specialised software (see Raup et al. 2014).

### 2.1.4. QA-GO-3: Outline overlay

If quantitative measures are not applicable, overlays of the outlines from different sources should be created and the differences in interpretation should be described.

### 2.1.5. QA-GO-4: Area variability

If the outlines from independent sources are comparable in quality and interpretation, sizes can be calculated for each individual glacier and outline dataset and a mean size and standard deviation can be provided as a measure of accuracy.

### 2.1.6. QA-GO-5: Area differences

If the different outline datasets show differences in interpretation, area differences can be small in total. By also determining omission and commission errors, a more realistic evaluation of data quality can be achieved.

### 2.1.7. QA-GO-6: Multiple digitizing

If outlines require intense manual correction (i.e. analyst intervention), the analyst(s) should digitize a few glaciers (5-10) with different sizes and debris cover *independently* 3-5 times. The standard deviation of the size variability gives a good estimate of dataset uncertainty.

### 2.1.8. QA-GO-7: Buffer

A final possibility to get at least a rough estimate of accuracy is to buffer the outlines by +/- ½ or 1 pixel, determine the resulting area differences and how large these are in a relative sense. This gives in most cases an upper bound estimate and requires neglecting internal boundaries (i.e. the assessment should be performed in raster space).

## 2.2. Elevation Change from DEM Differencing

### 2.2.1. Methods for validation

The end-to-end quality of the DEM differencing processing is assessed by analysing the differences in stable terrain where no temporal changes are expected. Combining DEMs of overlapping time periods assesses the temporal consistency of the elevation changes. Table 2.2 provides an overview of the tests that are described in more detail afterwards.

| Test | Description | Metrics |
|------|-------------|---------|
| QA-ECD-1 | DEM co-registration parameters | Linear translation coefficients in X, Y, and Z |
| QA-ECD-2 | Stable terrain test (after bias removal) | All slopes: mean, median, standard deviation, and RMSE, sample count; for slopes <20 degrees: mean, median, standard deviation, and RMSE, sample count |
| QA-ECD-3 | comparison with elevation changes from independent elevation data* | Mean, standard deviation, RMSE, sample count; histogram of difference between elevation change product and reference data set |

*Table 2.2: The quality test for DEM differencing. * when reference data are available*

Contract: 4000109873/14/I-NB
**Product Validation and Inter-comparison Report (PVIR)**

Name:     Glaciers_cci-D4.1_PVIR
Version:  1.6
Date:     21.12. 2017
Page:     7

### 2.2.2. QA-ECD-1: DEM co-registration shift parameters

The two DEMs used for calculating surface elevation changes, are co-registered by applying statistical fits derived from stable areas to determine the systematic horizontal and vertical offsets between the DEMs. These parameters provide an indication on the spatial coherency between the DEMs. Note: Large shift parameters do not indicate low quality DEM difference products. The parameters for co-registration are the linear translation coefficients in X-, Y- and Z-direction.

### 2.2.3. QA-ECD-2: Stable terrain test

The stationary (stable) area test is carried out after co-registration of the two DEMs and calculates the mean, standard deviation and RMSE for elevation differences derived from stable areas. For stable terrain we expect no difference between the DEMs. The quality parameters derived are the number of samples, mean, median, standard deviation, and RMSE of elevation differences, for all slopes, and for slopes below 20 degrees (as a typical threshold distinguishing flat from steep terrain).

### 2.2.4. QA-ECD-3: Intercomparison with elevation changes from independent datasets

This quality assessment test compares the surface elevation changes derived from different sources. In order to assess the quality of the product the reference elevation data set should have a significantly higher accuracy than the DEMs involved in the product generation. Potential reference data are time series of GPS measurements, airborne laser DEMs, and laser altimetry data (e.g. ICESat).

Critical issues for the DEMs to be used for intercomparison and cross-validation are spatial resolution (reference DEM resolution should be higher than the product to enable efficient resampling), accuracy (higher accuracy of reference data set than the product to be evaluated), and time lag (coincident period of reference dataset and product). The quality measures from the test include mean, standard deviation and RMSE of the difference between the surface elevation change of the product and the reference data set.

## 2.3. Elevation Change from Altimetry

This section describes the methods and tests for assessing the quality of surface elevation change products observed by altimetry.

### 2.3.1. Methods for validation

The method of deriving elevation change over time from altimetry was developed over flat regions such as ice sheets, and has been validated and used for science in such regions (e.g. Smith et al. 2009, Flament and Rémy, 2012). The terrain over ice caps is much more complex, which complicates the derivation method. Consequently, validation of new products over ice cap regions is important. Approaches for quality assessment are summarized in Table 2.3 and described in the following subsections.

| Test | Description | Parameters derived |
|------|-------------|--------------------|
| QA-ECA -1 | Inter-comparison with other satellite elevation change measurements | None |
| QA-ECA-2 | Inter-comparison with contemporaneous airborne elevation change measurements | Mean difference |

*Table 2.3: Overview of the quality tests for elevation change from altimetry.*


### 2.3.2. QA-ECA-1: Inter-comparison of satellite elevation change measurements

As a first order check, we inter-compare spatial patterns and magnitude of elevation changes from previous published altimetry studies over coincident regions. This allows for an initial and large scale assessment of the signals observed from CryoSat-2. For the Greenland and Antarctic GICs there are no satellite measurements that are contemporaneous to CryoSat-2 for exact comparisons.

### 2.3.3. QA-ECA-2: Inter-comparison with airborne elevation change measurements

We inter compare contemporaneous measurements of elevation change from CryoSat-2 and IceBridge ATM data in grid cells with coincident measurements. Examining statistics relating to the differences between the datasets assesses the bias between the two data sets.


## 2.4. Ice Velocity

This section describes the tests for assessment of the quality of the ice velocity products.

### 2.4.1. Overview of methods for validation

Ice velocity products are derived from various SAR sensors and from optical satellite data. Unless otherwise stated, when calculating statistics we refer to RGI 5.0 glacier outlines. With newer versions of the RGI or alternative glacier outlines, the statistics may vary. The methods for validation of flow velocities are summarized in Table 2.4 and described in the following.

| Test | Description | Measures of product quality |
|------|-------------|----------------------------|
| QA-IV-1 | Local measure of IV quality estimate, attached to the product | CC, SNR, None |
| QA-IV-2 | Fraction of area with valid IV measurements of total glacier area | % of total glacier area; Nr of data points |
| QA-IV-3 | Mean and RMSE of the velocity over stable terrain; mean values should be 0 | RMSE in East and North direction [m/day]; Mean difference (East, North [m/day]); Nr of data points |
| QA-IV-4 | Intercomparison with in-situ data | RMSE [m/day]; Mean difference (East, North [m/day]); Nr of data points |
| QA-IV-5 | Intercomparison of products from different sensors | as QA-IV-3 |

*Table 2.4: Overview of the quality test for the ice velocity product.*


### 2.4.2. QA-IV-1: Map local quality measures

Within the processing chain of the IV product generation local quality measures of the IV retrieval are estimated, like the Cross-Correlation coefficient (CC) and the signal to noise ratio

Contract: 4000109873/14/I-NB
Product Validation and Inter-comparison Report (PVIR)

Name: Glaciers_cci-D4.1_PVIR
Version: 1.6
Date: 21.12. 2017
Page: 9

(SNR). These measures quantify the quality of the local IV estimates and are attached to each product. They allow the user to select an appropriate threshold value for each case.

### 2.4.3. QA-IV-2: Coverage of IV measurements

This test calculates the coverage of valid IV measurements for the glacier area. This is given as fraction of the overall glacier area. For the statistics given here an arbitrary threshold is used on the correlation coefficients to determine valid measurements. The user should select an appropriate threshold value for each case. Unless otherwise stated, the glacier area is defined by the glacier outlines in the RGI 5.0.

### 2.4.4. QA-IV-3: Stable area test

Another internal method widely applied for quality assessment of velocity products is the analysis of stable ground where no velocity is expected. This gives a good overall indication for the bias introduced by the end-to-end velocity retrieval including co-registration of images, velocity retrieval, etc. After performing the matching for the entire region covered by the image pair, the results for the ice covered (moving) area will be separated from ice-free (stable) ground. The masking will be done using a polygon of the glacier outline. Buffers around the glacier polygon will be applied before extraction of stable ground for statistic calculation, or alternatively a final visual check for misclassified stable terrain will be performed in order to avoid potential errors introduced by the area polygon.

### 2.4.5. QA-IV-4: Intercomparison with in-situ data

The comparison of satellite derived velocity products with in-situ measured velocity data represents the highest level of validation. However, several issues complicate the comparison of space-borne glacier velocity estimates with in-situ data. Though highly precise, the temporal and spatial representativeness of the GPS data compared to the area and time covered by the image data to be validated will vary and is not strictly known. The comparison of in-situ GPS and satellite based IV products is done for each component separately (e.g. in map projection; note that velocity is given in true metres). For calculation of statistical parameters the number of in-situ data and corresponding EO observations has to be statistically significant.

### 2.4.6. QA-IV-5: Intercomparison of IV products from different sources

In general the product will be evaluated against a product derived from higher resolution data, which in general provides better quality of the velocity maps from offset tracking. Here we apply the comparison of velocity fields generated from independent data sets from different sensors covering the same period.

Contract: 4000109873/14/I-NB

**Product Validation and Inter-comparison Report (PVIR)**

Name: Glaciers_cci-D4.1_PVIR
Version: 1.6
Date: 21.12. 2017
Page: 10

# 3. Results of the Quality Assessment: Glacier Area

## 3.1. Product: Glacier Outlines Karakoram

### 3.1.1. Product description and data sets for intercomparison

In year 1 of Phase 2 we compared glacier outlines from different inventories for various parts of High Mountain Asia (HMA) that were provided recently as the second Chinese Glacier Inventory (CGI) for all of China (Guo et al. 2015), as the GAMDAM inventory for High Mountain Asia (Nuimura et al. 2015) and by ICIMOD (Bajracharya and Shrestha, 2011). We selected two key regions that are common to most of the datasets (Figs. 3.1 and 3.2). Table 3.1 provides details about each dataset. The tests performed are QA-GO-3 for the test region central Karakoram and QA-GO-4 for western Karakoram. Results for the latter are compiled in Table 3.2 and Figs. 3.2 and 3.3 while results for the first test are described in section 3.1.2.

| Dataset | Reference | Description | Identifier |
|---------|-----------|-------------|------------|
| CCI | Glaciers_cci | Automatically mapped and manually corrected | QA-Y1-CCI |
| CGI | Guo et al. 2015 | Automatically mapped and manually corrected | QA-Y1-CGI |
| ICIMOD | Bajracharya & Shrestha, 2011 | Manually and automatically digitized mostly from Landsat | QA-Y1-IM |
| GAMDAM | Nuimura et al. 2015 | Manually digitized from various sensors (ALOS, Landsat) | QA-Y1-GD |

*Table 3.1: Details of the datasets selected for QA-GO-4.*

### 3.1.2. QA-GO-3: Outline overlay

The visual comparison of the three glacier inventories shown in Figure 3.1 reveal rather small differences in the interpretation of ablation regions, debris-covered tongues and terminus positions. In part, differences are also due to surging glaciers that changed their extent over the variable reference periods. Overall, outlines from Glaciers_cci seem to be interpreted more generously than in the other two inventories. However, in the accumulation region the differences are often larger. While the position of the main drainage divide displays some variability, the largest differences are due to inclusion of seasonal snow at highest elevations and snow avalanche deposits on lower parts of the glacier tongue.

Moreover, it seems that very small ice/snow fields have only been considered in the Glaciers_cci inventory. Whether these have ice underneath or not, or are worth considering in an inventory or not is difficult to decide. From a practical point of view one can argue that it is always more easy to remove polygons (e.g. with a size threshold) than adding them. From the ICIMOD and GAMDAM inventories we have also learned that steep rock walls - whether covered by ice and snow or not - are generally excluded. This can also be seen in the examples of Figure 3.1 and Figure 3.2. We do not decide here if this is a good idea, but we emphasize that great caution has to be taken when the outlines are used for change assessment, mass balance/volume calculations and other glaciological applications. It is not possible to do this across datasets, as area differences due to interpretation can be much higher than area changes due to climate change (see also section 3.1.3).
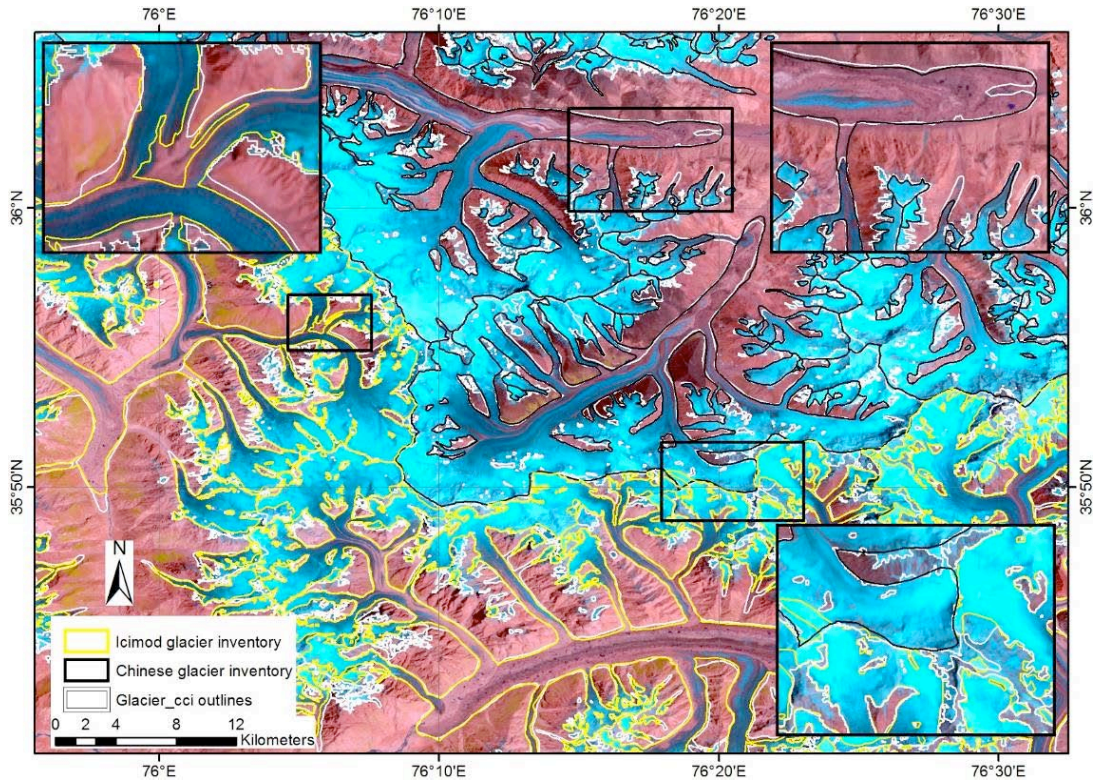
**glaciers cci**

Contract: 4000109873/14/I-NB

**Product Validation and Inter-comparison Report (PVIR)**

Name:     Glaciers_cci-D4.1_PVIR
Version:  1.6
Date:     21.12. 2017
Page:     11

*Figure 3.1: Overlay of glacier outlines for the central Karakoram for test QA-GO-3. Outlines from Glaciers_cci (white) are in the background, outlines from ICIMOD (yellow) and the CGI (black) are on top and cover different regions.*

### 3.1.3.  QA-GO-4: Area variability

For the results presented in Table 3.2 we investigated another region (depicted in Figure 3.2) were all three inventories overlap. For this region we additionally analysed the area-elevation distribution (hypsometry) in all inventories and for all glaciers (Figure 3.3). This comparison revealed an interesting change at 5700 m elevation. Below 5700 m, the area mapped in the ICIMOD and Glaciers_cci inventories are about the same while the CGI has mapped less area. Above 5700 m, the Glaciers_cci inventory has mapped more area than ICIMOD (green curve) but less than the CGI (red curve) so that the CGI considers even more area at these elevations than the Glaciers_cci inventory. Above 6200 m the latter has again the largest area mapped. As the CGI is also based on automated mapping of Landsat images rather than manual digitization, it is possible that this effect is due to unfavourable snow conditions at high elevations in the CGI (for this region). The relative differences get rather high above 6000 m as the total area covered (black curve) is strongly reduced. Although these numbers should not be over-interpreted, they reveal the high sensitivity of mapped glacier area at these elevations to image conditions.

| Inventory | Count | Area (km$^2$) | Diff. to CCI (%) | Mean elevation (m) | Diff. to CCI (m) |
|---|---|---|---|---|---|
| CCI | 49 | 59.9 | 0 | 5982.7 | - |
| CGI | 62 | 33.5 | -44.1 | 5945.3 | -37.4 |
| ICIMOD | 59 | 24.1 | -59.8 | 5917.3 | -65.4 |

*Table 3.2: Results of the tests QA-GO-4 for the region in Figure 3.2, Diff. is difference.*
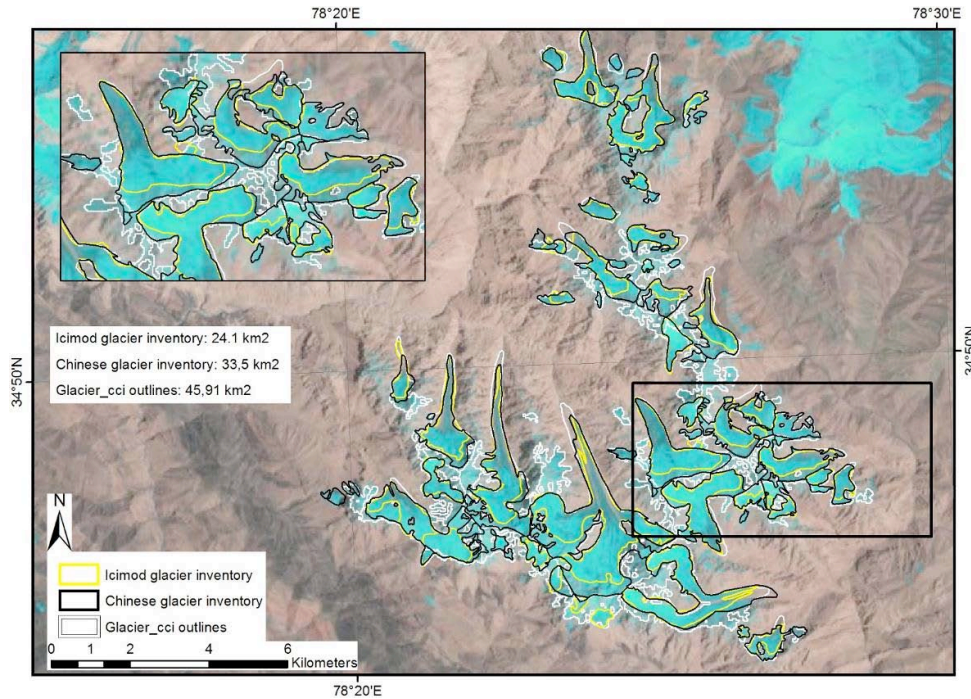
*Figure 3.2: Overlay of glacier outlines from the three inventories in the eastern Karakoram.*
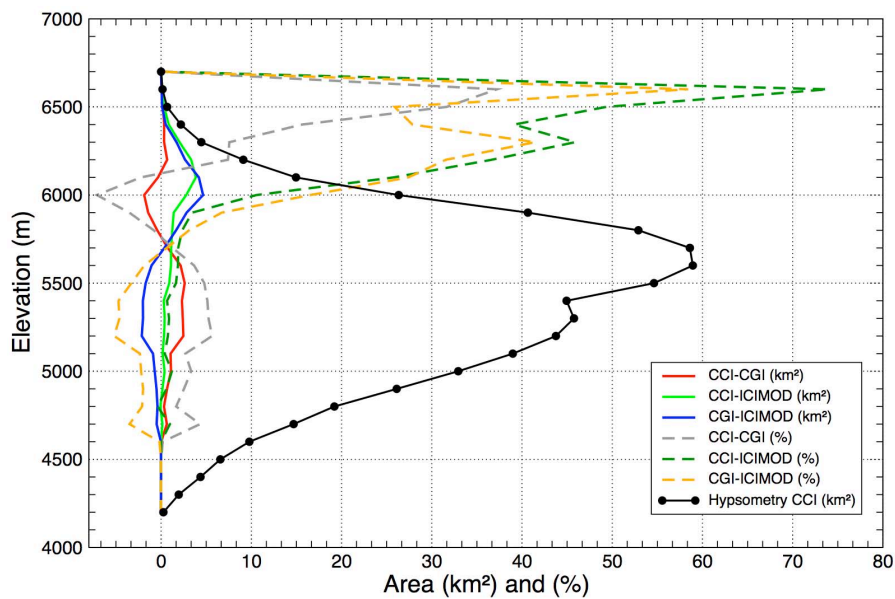


*Figure 3.3: Hypsometry of the CCI inventory along with absolute and relative area differences between the three inventories.*

Overall, the quality assessment across various glacier inventories reveals a strong dependence of results on image conditions (seasonal snow) and interpretation rules as applied by the analyst. Though there is some potential to harmonize and standardize the latter for the community, poor image conditions will always be a major obstacle in generating high quality results. Moreover, reporting of image conditions is not standardized, only partly done in related papers and even more rare in meta-data. This has to be improved in the future.

## 3.2. Glacier Outlines Hohe Tauern, Austria/Italy

### 3.2.1. Product description and data sets for intercomparison

We also compared glacier outlines generated by different classification methods applied on a subset of a Sentinel-2 scene of 13 August 2015 for selected glaciers of the Hohe Tauern mountain range, close to the border between Austria and Italy (Fig. 3). The scene was acquired during the commissioning phase of Sentinel-2, but has been reprocessed and fully recalibrated by ESA on 9 March 2016. The glacier outlines were generated automatically from the reprocessed scene for the intercomparison, without applying any manual correction for debris cover, water bodies, seasonal snow patches, cast shadow areas, or any other misclassified pixels (to avoid any impact of interpretation by the different analysts). Table 3.1 provides details about each dataset. We used the test QA-GO-3 for the preliminary glacier outlines. Results for this test are described and illustrated in section 3.2.2.

| Dataset | Reference | Description | Identifier |
|---|---|---|---|
| GIUZ | Glaciers_cci | Automatically mapped glacier outlines (thresholds manually selected but without manual corrections). | QA-Y2-CCI |
| ENVEO | Schwaizer et al. (2016) | Automatically mapped glacier outlines (thresholds manually selected but without manual corrections). | QA-Y2-ENV |

*Table 3.1: Details of the datasets selected for QA-GO-3.*

### 3.2.2. QA-GO-3: Outline overlay

The visual comparison of the two datasets is shown in Figure 3. for the entire study region and in Figure 3.5 for a subset. Already at the scale of Figure 3.4 large differences can be seen in the classification. The CCI algorithm is in general less strict than the one from ENVEO. The former includes small snow patches as well as most water bodies, while the latter has excluded such areas by applying more restrictive classification conditions, further band ratios and a filtering function removing small pixel clumps (<100 pixels) within the automated pre-processing line. On the other hand, due to fewer limitations, the CCI algorithm includes in general more snow and glacier areas than the ENVEO algorithm, especially for glacier ice in cast shadow and on debris-covered glacier areas. The band ratios and thresholds used for both algorithms can be adapted to include more (ENVEO) or less (CCI) of the snow and glacier areas, so that the results of both methods would result in a better match.

Such adaptations have not been further investigated as these would compromise the independent analysis of the original results. Moreover, it is also a matter of personal preference to edit in the post-classification stage more shadow/debris or water/snow fields. Whereas snow fields can be removed by applying a filter or size threshold, water can be classified with an additional band ratio (Huggel et al., 2002). Debris needs to be manually corrected in any case so that the shadow editing is the most demanding correction remaining for the ENVEO algorithm. Figures 3.4 and 3.5 illustrate the differences between both methods in detail.

Whereas the Glaciers_cci algorithm is based on digital numbers (scaled reflectance values) of Sentinel-2, the ENVEO algorithm applies a topographic correction on the rescaled top of atmosphere reflectance (TOAR) values of all bands used for the classification. Topographic information is obtained from the ASTER GDEM2 with 30 m cell size, resampled to 10 m. A different DEM, the PlanetDEM with 90 m pixel size, is used for the orthorectification of the

| | Contract: 4000109873/14/I-NB | Name: Glaciers_cci-D4.1_PVIR |
| | Product Validation and Inter-comparison Report (PVIR) | Version: 1.6 |
| | | Date: 21.12. 2017 |
| | | Page: 14 |

**glaciers cci**

Sentinel-2 Level 1C data. Accurate geolocation in steep, high-mountain terrain is challenging but very important, as topographic variability has a major impact illumination conditions. If a coarse resolution DEM, such as the PlanetDEM is used for orthorectification of a high resolution satellite data set (10 m in case of S2 VNIR bands) in such terrain, the wrong geolocation introduces errors in the detection of surface features, e.g. in steep valleys, and especially along mountain ridges and in cast shadowed areas
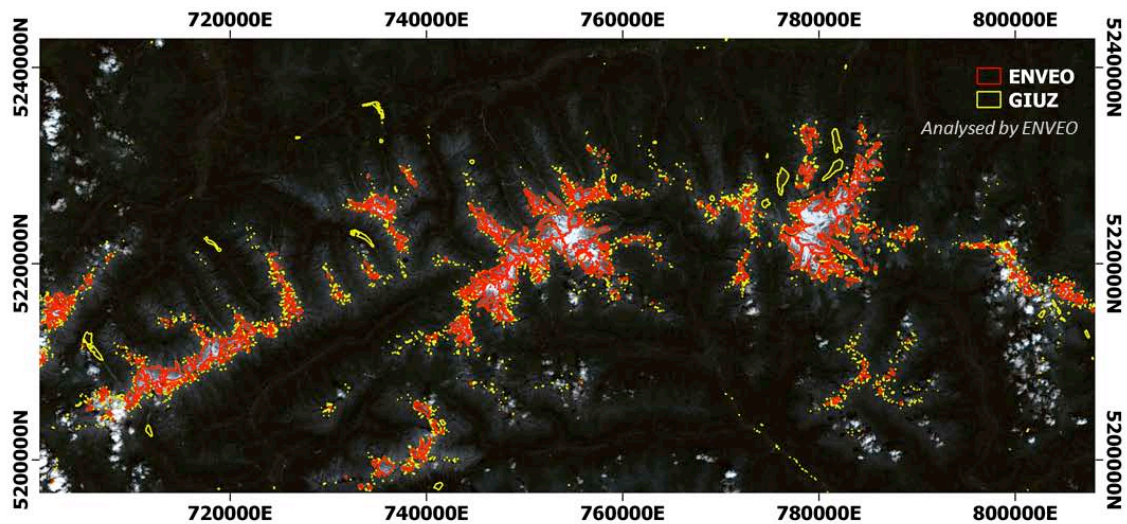


*Figure 3.4: Overlay of preliminary glacier outlines for the region Hohe Tauern, Austria/Italy for test QA-GO-3. The outlines from GIUZ (yellow) and ENVEO (red) are generated by applying different classification methods on the same Sentinel-2 scene from 13 August 2015.*
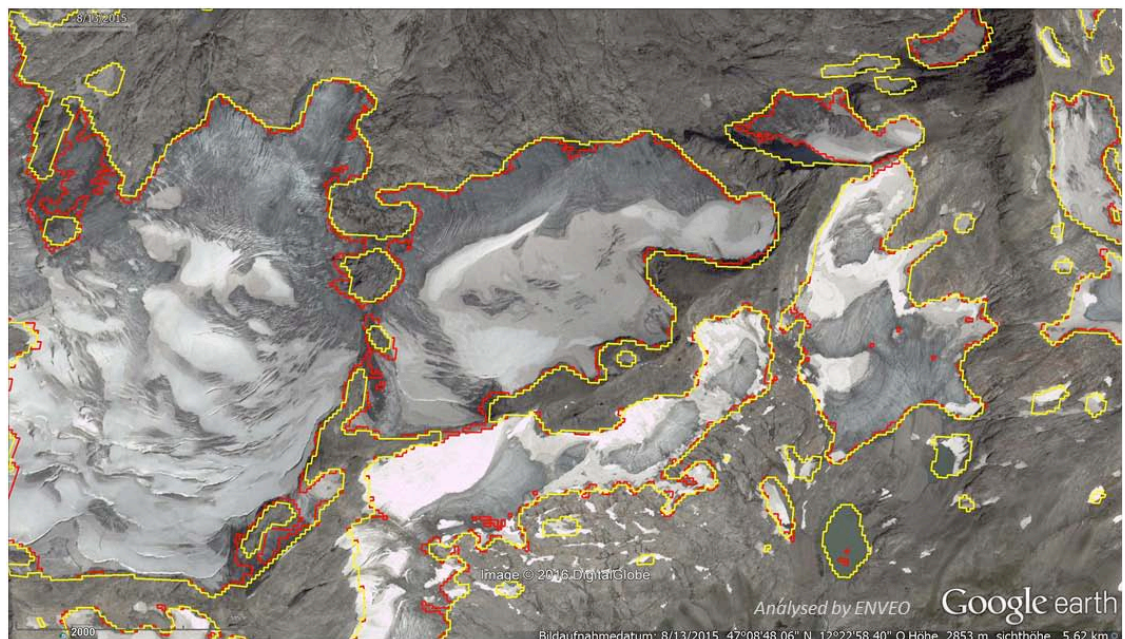


*Figure 3.5: Overlay of preliminary glacier outlines from GIUZ (yellow) and ENVEO (red) derived from the Sentinel-2 scene from 13 August 2015 on a Quickbird image of the same date.*

![glaciers cci logo]

Contract: 4000109873/14/I-NB
Product Validation and Inter-comparison Report (PVIR)

Name: Glaciers_cci-D4.1_PVIR
Version: 1.6
Date: 21.12. 2017
Page: 15

We have also tested how the ENVEO algorithm performs when DNs are used instead of topographically corrected TOAR values (Figure 3.6). Whereas there is little change for the larger glaciers, in particular a large amount of small snow fields are now included.
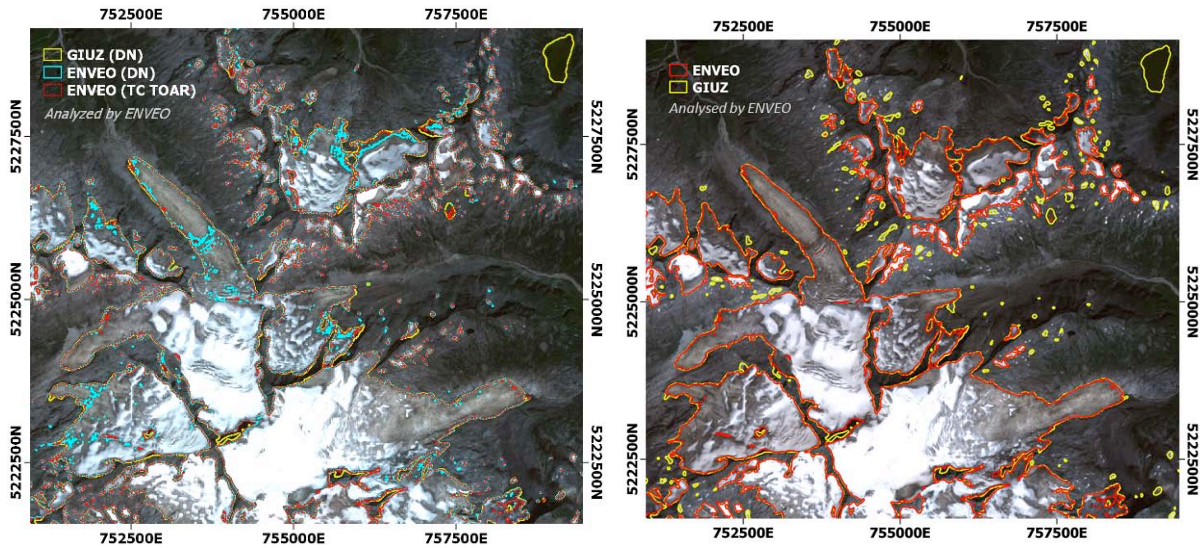


*Figure 3.6: Left: Comparison of intermediate glacier outlines from GIUZ using digital numbers (DNs, processed for CCI), and ENVEO from DNs and topographically corrected (TC) TOAR values (intermediate product of pre-processing chain). Right: resulting glacier outlines from the automated pre-processing chains from GIUZ and ENVEO.*

The evaluation of glacier outlines with reference data from other sources is challenging due to the limited data availability for the same date. Useful (i.e. snow free) high-resolution optical satellite data from sensors such as Quickbird or SPOT are available for some regions in Google Earth. Although these images are a great reference for visual checking, an overlay of glacier outlines from Sentinel-2 on the corresponding (same date) Quickbird scene in Google Earth show that there are locally strong shifts in geolocation (Figure 3.7).
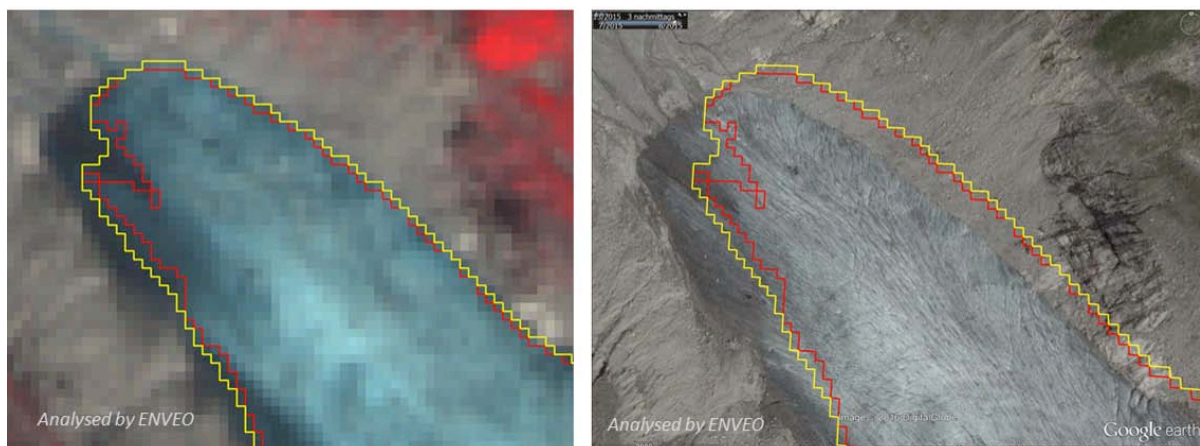


*Figure 3.7: Glacier outlines from GIUZ (yellow) and ENVEO (red) on a Sentinel-2 scene from 13.8. 2015 (left) and on the Quickbird image of the same date in Google Earth (right). The horizontal shift is about 65 m.*

glaciers cci

Contract: 4000109873/14/I-NB
Product Validation and Inter-comparison Report (PVIR)

Name:     Glaciers_cci-D4.1_PVIR
Version:  1.6
Date:     21.12. 2017
Page:     16

This geolocation shift is not constant but changes with the images available. For a time series of four images acquired between 2000 and 2015 we followed a fixed point on a moraine in stable terrain (Figure 3.7). Its change in position indicates that the respective images have been orthorectified differently (maybe with different DEMs or ground control points) and that the images in Google Earth can in general not be used as reference data set for geolocation.
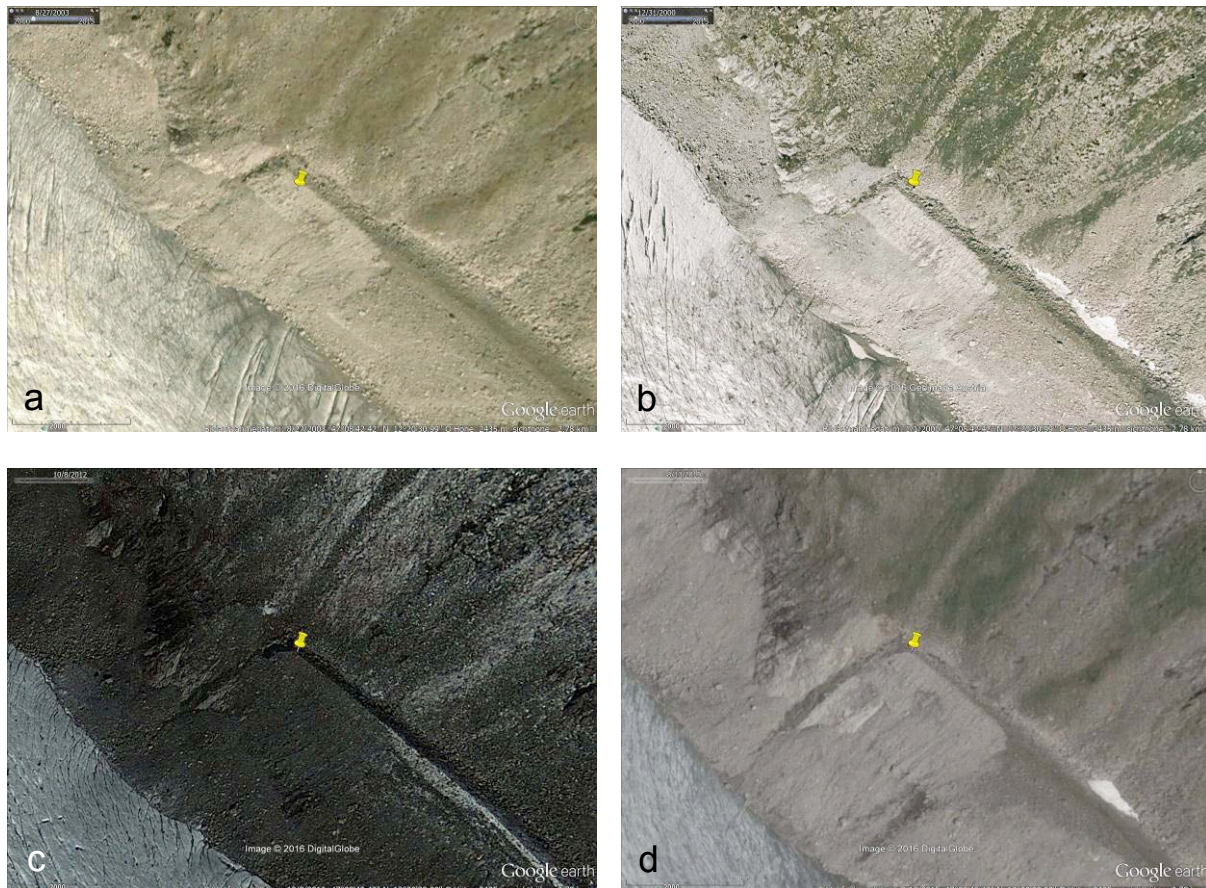


*Figure 3.8: Demonstration of geolocation inconsistencies of Quickbird images from different years as available in Google Earth. The yellow marker indicates a check point on top of a moraine crest in panel c and assumed to be nearly stable terrain. a) 27 August 2003, b) around July 2004 (exact date unknown), c) 08 October 2012, d) 13 August 2015.*

## 3.3. Glacier Inventory Novaya Zemlya

For the new glacier inventory covering Novaya Zemlya (Rastner et al. 2017) we have determined uncertainty with the buffer method (QA-GO-7) using a ±1/2 pixel buffer. As little debris cover was present, only few manual corrections were performed (mostly related to calving termini) and the multiple digitizing test (QA-GO-6) was not performed. Due to the different size distribution of glaciers in the northern and southern part of Novaya Zemlya, the calculated uncertainties of 0.5 and 4% (one standard deviation) were applied separately for the glaciers in the north and south, respectively. The mapped glacier areas were 20,784.4 ±103.9 $km^2$ for the northern part and 1612.6 ±64.5 $km^2$ for the southern part. In total, the derived area is 22,379 $km^2$ ±167.8 $km^2$.

xxx GIUZ results for Pamir/Karakoram to be added

# 4. Results of the Quality Assessment: Elevation Changes from DEM Differencing

## 4.1. DEM differencing

Accuracy assessment was performed for the elevation changes determined over glaciers in Svalbard comparing national with SPOT DEMs and for glacier No. 354 in the Tien Shan using two DEMs derived from Quickbird images (Kronenberg et al. 2016). The quality assessment of the new dataset for peripheral glaciers on Greenland (Korsgaard et al. 2016) will be provided with the next update of the document. The results for the two products mentioned above are summarized in Table 4.1.

xxx GUIO results from the Svalbard IDEM to be added

| Product ID in CRDP | Product description | QA-ECD-1 | | QA-ECD-2 (all slopes) | | QA-ECD-2 (slopes <20 deg) | | QA-ECD-3 |
|---|---|---|---|---|---|---|---|---|
| ECD_rgi7_001 | Svalbard surface elevation change from national DEMs and SPOT | X<br>Y<br>Z | -9.59 m<br>-6.37 m<br>4.30 m | Mean<br>Median<br>STD<br>RMSE<br>Nr samples | -0.24<br>-0.48<br>6.19<br>6.19<br>94684 | Mean<br>Median<br>STD<br>RMSE<br>Nr samples | -0.21<br>-0.44<br>4.88<br>4.88<br>73359 | N/A |
| ECD_rgi13_001 | Glacier 354 elevation change from Quickbird 2003-2011 | X<br>Y<br>Z | no systematic shift | N/A | | Mean<br>STD | -0.5<br>1.5 | -0.48 ±0.07 vs -0.4 ±0.1 m w.e. a$^{-1}$ (modelled) |

*Table 4.1: Summary of the quality assessment of elevation change products derived from DEM differencing (N/A: this test was not performed).*

## 4.2. DEM comparison

For a test site in western Greenland, where currently a new glacier inventory from Landsat 8 and Sentinel 2 is being created, a large number of DEMs are now available. Potentially, these can be used to derive elevation changes over glaciers, but foremost they are used to calculate drainage divides and topographic parameters for each glacier. This was formerly done with the freely available GIMP DEM (Howat and Negrete 2012) that is merged from the ASTER GDEMv1 and other topographic information (e.g. from SAR). The datasets now available include the AeroDEM, GIMP DEM, GDEMv2, ArcticDEM and the TanDEM-X DEM. Their characteristics are summarized in Table 4.2 and hillshades are compared in Figs. 4.1 and 4.2.

| DEM | Date | Cell size | Method | Sensor | Comments |
|---|---|---|---|---|---|
| AeroDEM | 1985 | 40 | Optical | Aerial | Large interpolation artefacts |
| GIMP | 2000-2010 | 90 | Opt.+InSAR | ASTER et al. | Bumpy surface, merged |
| GDEM v2 | 2000-2012 | 30 | Optical | ASTER | Smoothed bumps |
| ArcticDEM | 2007-2012 | 2/5 | Optical | Quickbird, WorldView | Large data voids, not yet useful |
| TanDEM-X | 2012-2014 | 12/30 | InSAR | TerraSAR-X, TanDEM-X | Provided by DLR proposal DEM_GLAC_xxx |

*Table 4.2: Characteristics of the DEMs available for Disko Island in western Greenland.*
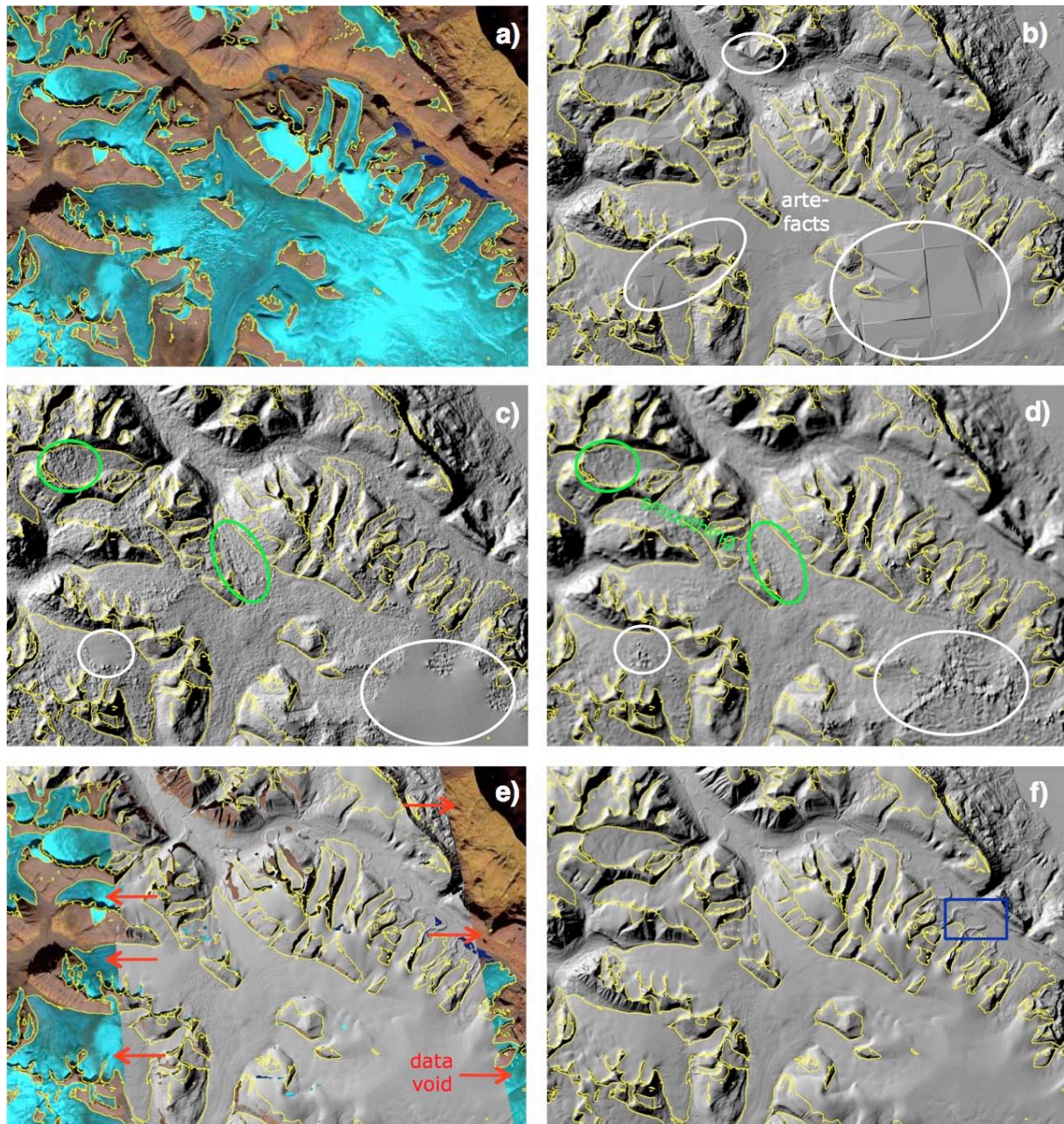
*Fig. 4.1: Comparison of five different DEMs for a test site on central Disko Island (western Greenland). a) The test site as seen on a Landsat 8 OLI false colour composite (bands 6, 5, 4 as RGB), b) AeroDEM, c) GIMP DEM, d) ASTER GDEM v2, e) Arctic DEM, and f) Tan-DEM-X DEM. White circles denote artefacts, green circles 'bumpy regions' in c) that have been smoothed in d) and red arrows in e) point to large data voids. The region in the blue square in f) is magnified in Figure 4.2. See text for discussion and Table 4.2 for DEM details.*

The AeroDEM from 1985 (Fig. 4.1b) shows high spatial detail but suffers from partly large triangular-shaped interpolation artefacts in steep terrain as well as over flat glacier surfaces. The GIMP DEM (Fig. 4.1c) shows strongly smoothed surfaced where the ASTER GDEM has artefacts (white circles in Fig. 4.1d). It can also be seen that the GIMP DEM is largely based on the original ASTER GDEM (v1) in this region that has much more pronounced 'bumps'

over glacier surfaces (green circles in Fig. 4.1c). These have been strongly smoothed in GDEM v2 (Fig. 4.1d) but the strong interpolation artefacts are back (white circles). The Arc-ticDEM in Fig. 4.1e (5 m mosaic) shows extremely fine details, but it is only available for some stripes (covering glaciers only partly) and can thus not yet be used in this region. The TanDEM-X DEM (Fig. 4.1f) shows somewhat less spatial detail than the AeroDEM and is less detailed than the ArcticDEM. However, it covers the entire region completely and shows no interpolation artefacts. It has thus been decided to use this DEM to derive drainage divides and topographic parameters for the new inventory.

The sub-sets of the lake-filled terminal moraine shown in Fig. 4.2 confirm the differences described above. The strong smoothing of the GDEM compared to v1 can be well followed in Figures 4.2c and b, respectively. Also the very fine spatial detail visible in the ArcticDEM (5 m resolution version) in Fig, 4.2e is well recognizable when compared to the AeroDEM and TanDEM-X DEM in Figures 4.2 d) and f), respectively. Once spatially complete, the Arc-ticDEM will certainly completely revolutionize geomorphometric applications. Until then, the TanDEM-X DEM is the best choice for the region.
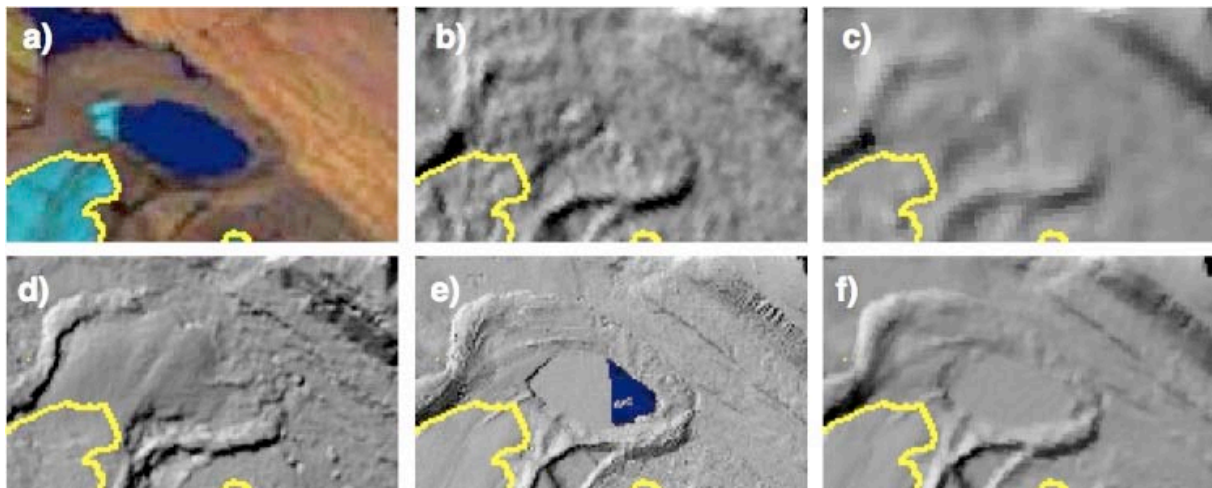


*Fig. 4.2: Comparison of five different DEMs for a subset of the test site on central Disko Island presented in Fig. 4.1. a) The subset as seen on a Landsat 8 OLI false colour composite (bands 6, 5, 4 as RGB), b) GIMP DEM, c) ASTER GDEM v2, d) AeroDEM, e) Arctic DEM, and f) TanDEM-X DEM. See text for discussion and Table 4.2 for DEM details.*

As expected, the drainage divides derived from the TanDEM-X DEM (black in Fig. 4.3) are partly located at different places than those derived from the GIMP DEM (red in Fig. 4.3) for the glacier inventory by Rastner et al. (2012). Moreover, they are smoother than those derived from the GIMP DEM. The shift of the divides has a small impact on the overall size distribution of glaciers, but a larger one on glacier-specific topographic parameters (e.g. mean slope and aspect or mean and maximum elevation) and potential modelling applications.

We have finally also investigated if DEM differencing is providing any useful elevation change values over glaciers. For this purpose we have subtracted the AeroDEM from 1985 from the TanDEM-X DEM acquired around 2013 (Figures 4.4 and 4.5). The related colour-coded difference image for central Disko Island reveals several interesting changes.

Contract: 4000109873/14/I-NB

**Product Validation and Inter-comparison Report (PVIR)**

Name: Glaciers_cci-D4.1_PVIR
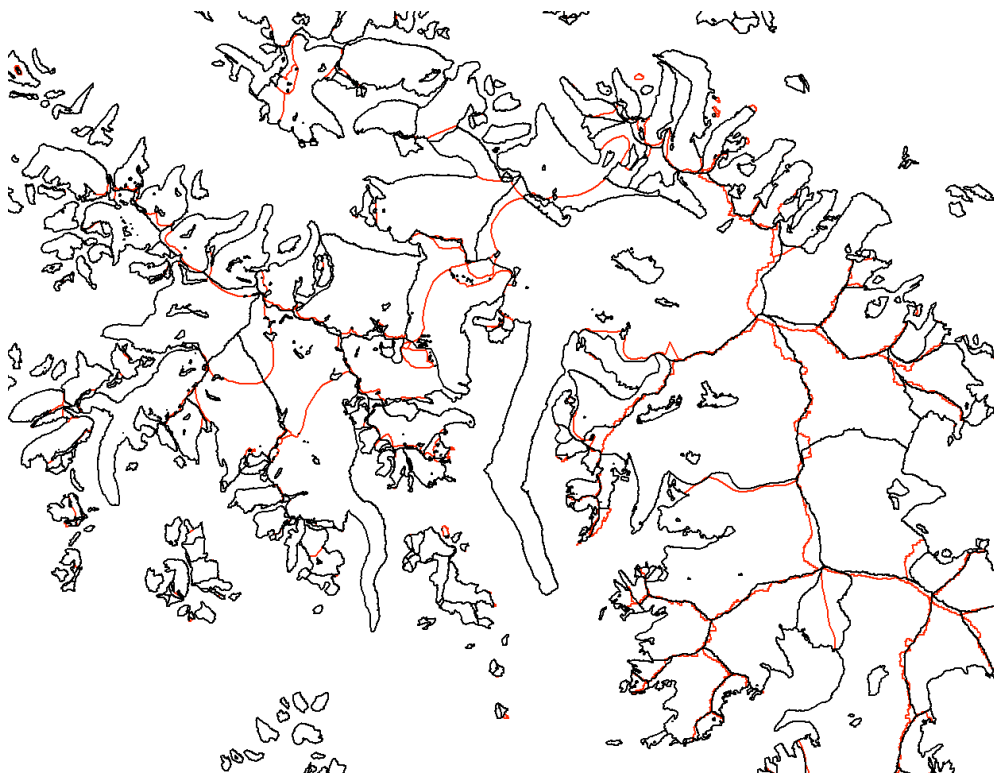Version: 1.6
Date: 21.12. 2017
Page: 20

*Figure 4.3: Glacier outlines for central Disko Island and comparison of drainage divides derived from the TanDEM-X DEM (black) compared to those in the current glacier inventory for Greenland (Rastner et al. 2012) derived from the GIMP DEM (red).*
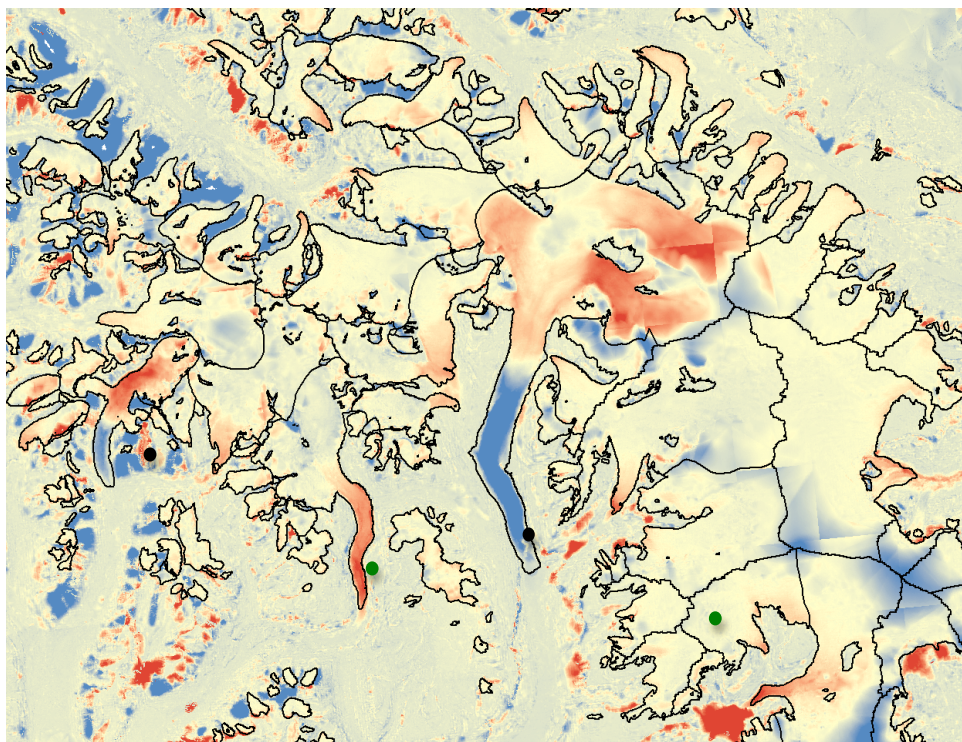


*Figure 4.4: Elevation changes from 1985 to ~2013 from differencing the AeroDEM from the TanDEM-X DEM for central Disko Island in western Greenland. The main changes are described in the text. From blue to red values range from +150 to -150 m.*

**Contract:** 4000109873/14/I-NB

Product Validation and Inter-
comparison Report (PVIR)

Name: Glaciers_cci-D4.1_PVIR
Version: 1.6
Date: 21.12. 2017
Page: 21

Most striking are the strong elevation changes taking place for three surge-type glaciers. Strong elevation loss in the accumulation region (red) can be well distinguished from a related elevation gain in the ablation region (blue) for the two glaciers that have surged between 1985 and 2000 (marked by black dots). Between them and in the lower right of the image one can see two completely red glacier tongues (green dots). These glaciers are in their post-surge down-wasting (or quiescent) phase for the full time since 1985. It is very likely that all of these changes are correctly captured. On the other hand, two kinds of artefacts can be seen: One is resulting from the triangular interpolation artefacts over flat regions of glaciers (marked in Fig. 4.1b) and those being just outside of glaciers with a more concentrated shape (most of them are dark blue, i.e. the TanDEM-X DEM is more than 150 m higher in these regions). These massive differences occur mostly in steep, but otherwise stable terrain. Any accuracy assessment in these regions would reveal very high uncertainties that would even make the strongest elevation changes (of the surge-type glaciers) too uncertain to be significant.

To obtain a clearer picture of the real uncertainties, it is required to select regions of stable terrain outside these artefact regions. The third observation is that here elevation differences are very small so that again the more subtle elevation changes (outside the triangular arte-facts) become significant again. This allows us to also consider the limited lowering of re-treating glacier tongues in the northeast and the correct elevation gain of an advancing glacier in the upper centre as correct. Not unlikely is the small but homogenous elevation gain of glaciers in the left centre (north of the constantly retreating surge-type glacier) correct. So at some point these glaciers might start surging again (but periodicity is not yet known). The se-cond example depicting the western Nuussuaq Peninsula (Fig. 4.5) shows basically the same trends. Massive over and underestimations of elevation changes are visible on and off glaciers so that the more subtle changes would be doubtful. Again, however, in flat terrain outside of glaciers the differences are very small so that even subtle changes might be relevant. And here the blue and red patterns of some larger glaciers to the west of the centre show a highly varia-ble pattern: four are showing elevation gain near the terminus and lowering higher up (i.e. they are advancing or have been surging) and four show surface lowering near the terminus.
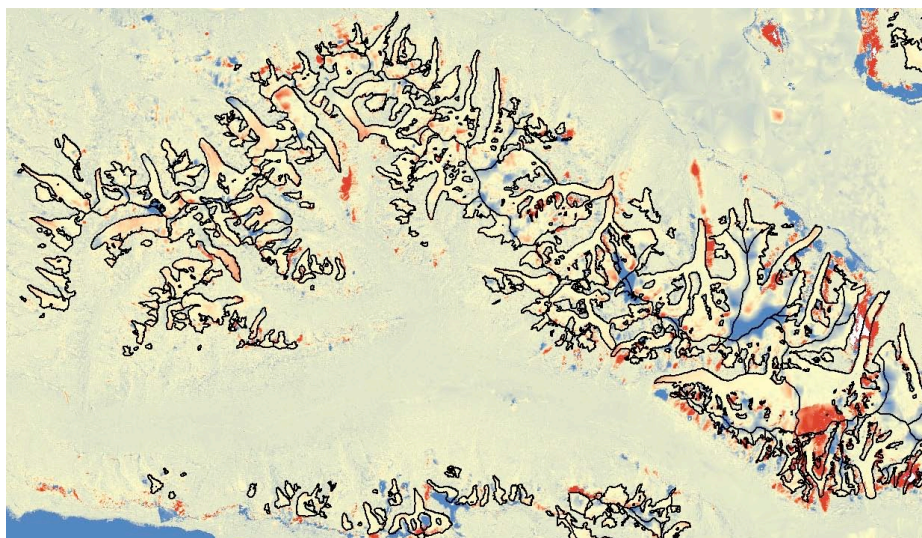


*Figure 4.5: Elevation changes from 1985 to ~2013 from differencing the AeroDEM from the TanDEM-X DEM for the western part of the Nuussuaq peninsula in western Greenland. The main changes are described in the text. From blue to red values range from +150 to -150 m.*

Contract: 4000109873/14/I-NB

Product Validation and Inter-
comparison Report (PVIR)

glaciers
cci

Name: Glaciers_cci-D4.1_PVIR
Version: 1.6
Date: 21.12. 2017
Page: 22

# 5. Results of the Quality Assessment: Elevation Changes from Altimetry

## 5.1. Product: CryoSat-2 elevation change of Greenland ice caps

### 5.1.1. Product Description

Below, we provide an overview of the validation performed on CryoSat-2 (CS2) elevation change measurements using IceBridge ATM data over ice caps in Greenland.

### 5.1.2. Reference Validation Data

We use data from repeat IceBridge flight lines between 2010 and 2014. Elevation change is estimated by differencing point measurements that are within 10 m of each other.

### 5.1.3. Results of *QA-ECA-2*

For a comparison of the datasets, we gridded the ATM elevation change measurements onto the same 2x2 km grid used for the CryoSat-2 measurements (Figure 5.1, left). We filtered the ATM measurements to remove grids containing fewer than 10 measurements and exceeding 1 m/yr standard deviation. This left 242 grid cells that were coincident with the CryoSat-2 measurements. We found a mean difference between the ATM and CryoSat-2 elevation change rate estimates of -4 cm/yr (Figure 5.1, right).



*Figure 5.1: Validation of Greenland GIC CryoSat-2 SEC with IceBridge ATM SEC measurements. The image to the left shows the spatial distribution of the elevation change difference measurements from Cryosat-2 and ATM. Top right is a zoom of these differences over Flade Isblink Ice Cap in the NE of Greenland. In grey, is the coverage of GICs based on the GLIMS definition. The graph on the bottom right is a histogram showing the statistical distribution of the differences between the ATM and CryoSat-2 elevation change rates.*

![glaciers cci logo]

| | | | |
|---|---|---|---|
| | Contract: 4000109873/14/I-NB | Name: | Glaciers_cci-D4.1_PVIR |
| | Product Validation and Inter- | Version: | 1.6 |
| | comparison Report (PVIR) | Date: | 21.12. 2017 |
| | | Page: | 23 |

# 6. Results of the Quality Assessment: Ice Velocity

The quality tests for ice velocity (IV) products are described in Section 2.4. Table 6.1 below lists all IV products available in the CRDP and provides an overview on the QA tests carried out for each data set. Because QA-IV 1 (CC/SNR), 2 (per cent coverage of area), and 3 (RMSE for ice-free regions) are already recorded in the metadata of each generated product and the number of products in the CRDP is steadily increasing, starting from Year 2 on we here only present selected examples of these tests that should form a representative sample of all cases encountered. Selected results of the quality assessment for QA-IV 4 (in-situ data) or QA-IV 5 (products from different sources / sensors) or for particular situations are only presented when suitable reference / validation data are available. The validation and quality assessment results described in this chapter include IV products from all regions of interest, covering different glacier types and acquired by multiple sensors (e.g. ALOS PALSAR, Sentinel-1 & TerraSAR-X). They are therefore considered to be representative.

| Product ID in CRDP | Product description | Applied QA-IV Tests | Section Number |
|---|---|---|---|
| IV_rgi14_005 | Ice velocity maps for RGI region 14, covering the Karakorum mountain range, derived from TSX images, from different periods between 2011 and 2014 | 1,2,3 | Section 6.1 |
| IV_rgi14_006 | Ice velocity maps for RGI region 14 covering the Karakoram mountain range, derived from ALOS PALSAR FBS images from different periods between 2008 - 2010 | 1, 2, 3 | Section 6.2 |
| IV_rgi14_007 | Ice velocity maps for RGI region 14 covering the Karakoram mountain range, derived from ALOS PALSAR FBD images from different periods between 2007 - 2009 | 1, 2, 3 | Section 6.3 |
| IV_rgi03_004/5 | Ice velocity maps for RGI region 3 covering the Ellesmere and Devon ice caps, derived from ALOS PALSAR FBS images from different periods between 2007 and 2011 | 1, 2, 3 | |
| IV_rgi03_001/2 /6/7/8 | Ice velocity maps for RGI region 3 covering the Ellesmere and Devon ice caps, derived from Sentinel-1 images from January and February 2015 | 1, 2, 3 | |
| IV_rgi03_009 | Ice velocity maps for RGI region 3 covering the Ellesmere and Devon ice caps, derived from Sentinel-1 images from February and March 2016 | 1, 2, 3 | |
| IV_rgi04_001 | Ice velocity maps for RGI region 4 covering the Baffin ice cap, derived from ALOS PALSAR FBS images from different periods between 2007 and 2011 | 1, 2, 3 | |
| IV_rgi04_002/3 | Ice velocity maps for RGI region 4 covering the Baffin ice cap, derived from Sentinel-1 images from Jan to Mar 2016 | 1, 2, 3 | |
| IV_rgi07_002/3 | Ice velocity maps for RGI region 7 covering the Svalbard Archipelago, derived from ALOS PALSAR FBD/FBS images from different periods between 2007 and 2011 | 1, 2, 3 | |
| IV_rgi07_004 | Ice velocity maps for RGI region 7 covering the Svalbard Archipelago, derived from TerraSAR-X images from different periods in 2008 and 2012 | 1, 2, 3 | |
| IV_rgi07_001 | Ice velocity maps for RGI region 7 covering the Svalbard Archipelago, derived from Sentinel-1 images from different periods between January and February 2015 | 1, 2, 3, 4 | Section 6.4 |
| IV_rgi09_001 | Ice velocity maps for RGI region 9 covering Novaya Zemlya, derived from ALOS PALSAR FBS images from different periods between 2008 and 2010 | 1, 2, 3 | |

| Product ID in CRDP | Product description | Applied QA-IV Tests | Section Number |
|---|---|---|---|
| IV_rgi09_002 | Ice velocity maps for RGI region 9 covering Novaya Zemlya, derived from Sentinel-1 images from different periods between September and October 2015 | 1, 2, 3 | |
| IV_rgi09_003 | Ice velocity maps for RGI region 9 covering Franz-Josef Land, derived from Sentinel-1 images from different periods in October 2015 | 1, 2, 3 | |
| IV_rgi13_005 | Ice velocity maps for RGI region 13 covering the Pamir mountain range, derived from ALOS PALSAR FBD images from different periods in 2007 | 1, 2, 3 | |
| IV_rgi13_004 | Ice velocity maps for RGI region 13 covering the Pamir mountain range, derived from ALOS PALSAR FBS images from different periods between 2009 and 2010 | 1, 2, 3 | |
| IV_rgi13_001 | Ice velocity maps for RGI region 13 covering the Pamir mountain range, derived from Sentinel-1 images from different periods between March and July 2015 | 1, 2, 3 | |
| IV_rgi14_008 | Ice velocity maps for RGI region 14 covering the Karakoram mountain range, derived from ENVISAT ASAR images from different periods between 2004 and 2005 | 1, 2, 3 | |
| IV_rgi14_001-4 | Ice velocity maps for RGI region 14 covering the Karakoram mountain range, derived from Sentinel-1 images from different periods between Feb and Aug 2015 | 1, 2, 3 | |
| IV_rgi19_001 | Ice velocity maps for RGI region 19 covering South Georgia, derived from ALOS PALSAR FBD images from different periods between May and July 2010 | 1, 2, 3 | |
| iv_rgi19_002 | Ice velocity map for RGI region 19 covering South Georgia derived from TSX images acquired in June-July 2013 | 1,2,3 | Section 6.5 |
| iv_rgi19_003 | Ice velocity maps for RGI region 19 covering South Georgia, derived from ALOS PALSAR FBD images from different periods between May and July 2010 | 1,2,3 | Section 6.5 |
| iv_rgi19_004 | Ice velocity map for RGI region 19 covering Alexander Island, derived from Sentinel-1 images from 2014-2016 | 2,3,5 | Section 6.6 |
| iv_rgi19_005 | Ice velocity map for RGI region 19 covering Alexander Island, derived from ALOS PALSAR images from 2010 | 2,3,5 | Section 6.7 |
| iv_rgi19_006 | Ice velocity maps for RGI region 19 covering South Georgia, derived from Sentinel-1 images from Jul-Sep 2016 | 2,3 | Section 6.8 |
| iv_rgi07_006 | Ice velocity maps for RGI region 7 covering the Svalbard Archipelago, derived from Sentinel-1 images from 2015-2017 | 2,3 | Section 6.9 |

*Table 6.1: Overview of products for which quality assessment is carried out. For some datasets detailed examples are shown in the sections indicated.*

## 6.1. Product: Ice Velocity Karakoram TSX (ID: IV_rgi14_005)

### 6.1.1. Product description and summary of quality assessment tests

The data sets provide ice velocity of glaciers in the Karakoram region. The ice velocity is derived by SAR offset tracking using TerraSAR-X image pairs acquired in stripmap mode between 2011 and 2014. The offset tracking algorithm performs iterative template matching with a variable window size to allow shearing zones and spatial variation of glacier velocity to be resolved better. The data sets are comprised of compressed ASCII tables (csv format) listing velocity components (E, N & vertical) converted to metres per day ([m/d]) and correla-

tion coefficients with results in geographic (Lat/Lon) projection. The vertical velocity is derived from the interpolated height at the end position of the displacement vector minus the elevation at the start position, as taken from the SRTM v4 DEM. The data products are gridded at ~28m (0.00025°) and include an xml file (metadata) and a quicklook image.

### 6.1.2. Reference validation dataset

No validation data (in-situ or from other sensors) are available for the region and time period of the generated IV products at the time of writing. The Karakoram TSX derived IV products maps are therefore presented with correlation coefficients produced by the FT matching algorithm as a local quality measure. In addition, we provide an overview, including maps, illustrating the coverage of successful IV measurements for selected glaciers and successful coverage percentage per product. Finally, we present an analysis of the algorithm performance in stable regions. A summary of the performed tests and outcome is given in Table 6.2.

| Track | QA-IV-1 [CC/SNR] | QA-IV-2 [% coverage of area] | QA-IV-3 [Mean, RMSE in m/d] | | QA-IV-4 | QA-IV-5 |
|---|---|---|---|---|---|---|
| | | | **East** | **North** | | |
| 7 | CC | 97.8 | 0.00, 0.05 | 0.00, 0.05 | N/A | N/A |
| 75 | CC | 93.6 | 0.00, 0.05 | 0.01, 0.07 | N/A | N/A |
| 75 | CC | 93.3 | 0.00, 0.04 | 0.01, 0.06 | N/A | N/A |
| 98 | CC | 95.2 | -0.04, 0.10 | 0.00, 0.07 | N/A | N/A |
| 151 | CC | 97.2 | 0.00, 0.03 | 0.00, 0.03 | NA | NA |

*Table 6.2: Quality assessment of IV products available in the product container glaciers_cci_iv_rgi14_TSX_2011-2014_v150814.zip. The performed tests are described in more detail in Section 6.1.3. QA-IV-4 and QA-IV-5 were not performed for the listed datasets.*

### 6.1.3. Results of QA tests

#### 6.1.3.1. QA-IV-1: Correlation coefficients of measurements

Figure 6.1 shows Cross-Correlation Coefficients (CC), a measure of the correlation strength of matching image templates, produced by the FT matching algorithm. The FT algorithm rejects all matches with a CC lower than 0.05. The CC is included with the IV products and allows the user to select an appropriate threshold value for each case.

#### 6.1.3.2. QA-IV-2: Coverage of IV measurements

Table 6.3 gives an overview of the glacierized area and the percentage coverage of successful ice velocity measurements for each individual scene/product. For the glacier area the latest release of the Karakoram glacier inventory from GIUZ is used available from the Glaciers_cci CRDP2 database (glaciers_cci_gi_rgi14s02_TM-ETM_1998-2002_v150505) and also included in RGI 5.0. This dataset is based on automated mapping and manual editing of Landsat scenes from the period 1998–2002. Apart from some actively surging glaciers with strong frontal changes, glacier extents are rather stable in the Karakoram so these extents can still be used. Any areal changes that have occurred since this period in general only slightly affect the IV coverage percentage. Figure 6.2 and Table 6.4 show IV maps and the percentage coverage of valid velocity measurements for selected glaciers. This is given as fraction of the total area for each glacier.

glaciers cci

Contract: 4000109873/14/I-NB
Product Validation and Inter-
comparison Report (PVIR)

Name:      Glaciers_cci-D4.1_PVIR
Version:   1.6
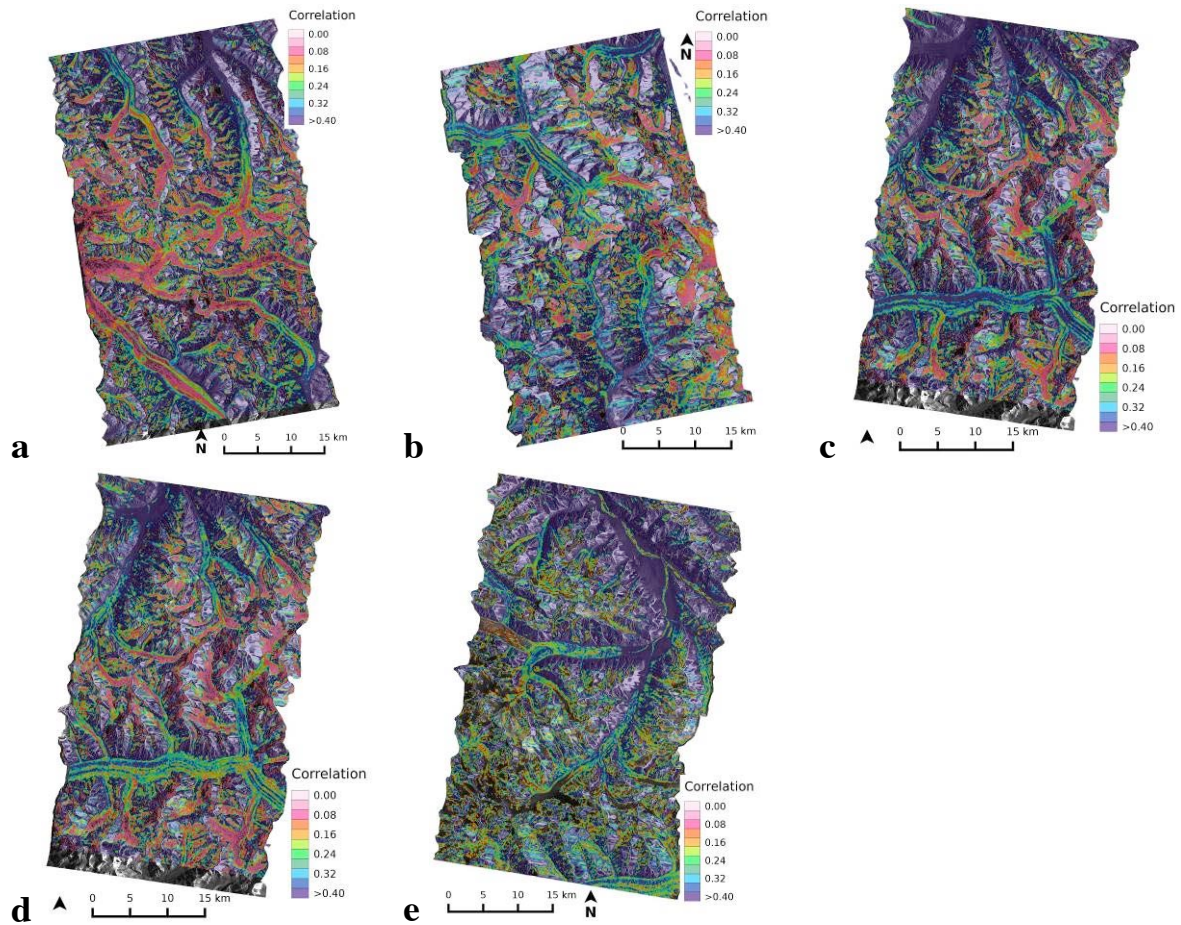Date:      21.12. 2017
Page:      26

*Figure 6.1: Maps of correlation coefficients for each of the TSX derived IV products: a) track 7 (IV-001-1), b) track 98 (IV-001-4), c) track 75 2011 (IV-001-2), d) track 75 2014 (IV-001-3), e) track 151 (IV-001-5).*

| Date 1 | Date 2 | Glacier Area [km$^2$] | IV Area [km$^2$] | Coverage [%] |
|---|---|---|---|---|
| 20131011 | 20131102 | 1292 | 1264 | 97.8 |
| 20111112 | 20111204 | 882 | 825 | 93.6 |
| 20140410 | 20140524 | 882 | 822 | 93.3 |
| 20141004 | 20141015 | 1124 | 1070 | 95.2 |
| 20120909 | 20121125 | 998 | 970 | 97.2 |

*Table 6.3: Total glacier area, IV area and percentage of coverage for velocity products.*

| Date 1 | Date 2 | Glacier Name | Area [km$^2$] | Coverage [%] |
|---|---|---|---|---|
| 20131011 | 20131102 | Bulaerdu | 176 | 100 |
|  |  | Hurdopin | 203 | 17 |
| 20111112 | 20111204 | Baltoro | 806 | 53 |
|  |  | Gasheluomu | 108 | 10 |
|  |  | Musita | 199 | 49 |
|  |  | Qiaogeli | 94 | 98 |

| Date 1 | Date 2 | Glacier Name | Area [km$^2$] | Coverage [%] |
| --- | --- | --- | --- | --- |
| 20140410 | 20140524 | Baltoro | 806 | 53 |
| | | Gasheluomu | 108 | 11 |
| | | Musita | 199 | 47 |
| | | Qiaogeli | 94 | 98 |
| 20141004 | 20141015 | Baltoro | 806 | 41 |
| | | Gasheluomu | 108 | 79 |
| | | Wuerduoke | 81 | 62 |
| 20120909 | 20121125 | Baltoro | 806 | 22 |
| | | Musita | 199 | 92 |
| | | Qiaogeli | 94 | 31 |
| | | Yinsugaiti | 393 | 47 |

*Table 6.4: Glacier area and percentage coverage in IV products for selected glaciers. The numbers serve as guidance for selecting the most useful product for a particular glacier.*
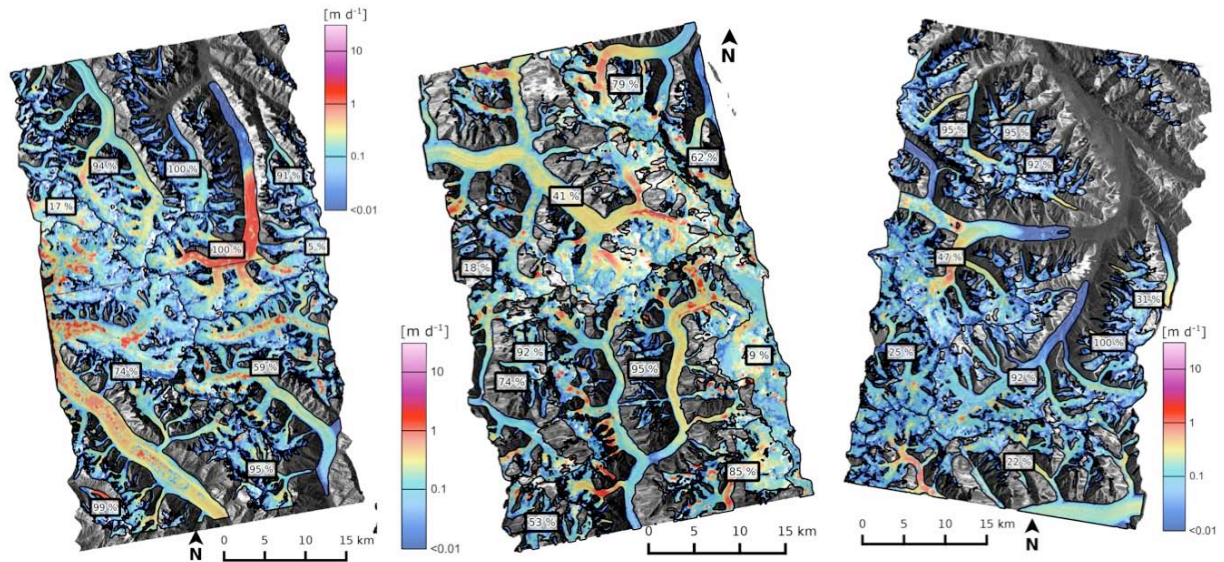


*Figure 6.2: Maps showing IV for tracks 7 (IV-001-1), 98 (IV-001-4) and 114 (IV-001-5) and coverage (%) of IV measurements for selected glaciers (background: TSX amplitude image).*

### 6.1.3.3. QA-IV-2: Stable ground test

The stable ground test is carried out for all IV velocity products (Figs. 6.3 to 6.5 and Table 6.5). To identify regions without motion (stable ground) vector outlines of rocks from the GLIMS database (Raup et al. 2007) are used. The red labelled areas depicted on the TerraSAR-X amplitude images in the figures show the stable areas for which the analysis is performed. Layover regions are masked out and are excluded from the statistical calculations. Scatter plots and histograms are presented illustrating the distribution of the easting and northing velocity components. Ideally these should be centred close to zero for stable areas, the statistical parameters that quantify this are the mean and RMSE. The RMSE is a measure of accuracy and represents the sample standard deviation of the residuals. Deviations can be due to several causes including errors in the rock shapefile, errors in the layover mask and ar-

Contract: 4000109873/14/I-NB

**Product Validation and Inter-comparison Report (PVIR)**

Name: Glaciers_cci-D4.1_PVIR
Version: 1.6
Date: 21.12. 2017
Page: 28

tefacts produced by the algorithm. The outcome of the stable ground test are very favourable showing on average a mean of -0.01 m d$^{-1}$ and 0.00 m d$^{-1}$ and an RMSE of 0.05 m d$^{-1}$ and 0.06 m d$^{-1}$ for respectively the easting and northing components (Table 6.5). The values depicted therefore indicate the mean 'velocity' in stable terrain and standard deviation of the residuals in m/day.

| Product ID | Date 1 | Date 2 | Number of pixels | Mean E [m d$^{-1}$] | RMSE E [m d$^{-1}$] | Mean N [m d$^{-1}$] | RMSE N [m d$^{-1}$] |
|---|---|---|---|---|---|---|---|
| IV-001-1 | 20131011 | 20131102 | 284,193 | 0.00 | 0.05 | 0.00 | 0.05 |
| IV-001-2 | 20111112 | 20111204 | 206,745 | 0.00 | 0.05 | 0.01 | 0.07 |
| IV-001-3 | 20140410 | 20140524 | 204,415 | 0.00 | 0.04 | 0.01 | 0.06 |
| IV-001-4 | 20141004 | 20141015 | 273,181 | -0.04 | 0.10 | 0.00 | 0.07 |
| IV-001-5 | 20120909 | 20121125 | 265,601 | 0.00 | 0.03 | 0.00 | 0.03 |
| Mean over all products | | | - | **-0.01** | **0.05** | **0.00** | **0.06** |

*Table 6.5: Summary of stable rock quality assessment for TSX derived velocities in the Kara-koram. The bias in easting direction in IV-001-4 is possibly related to glitches in the DEM.*
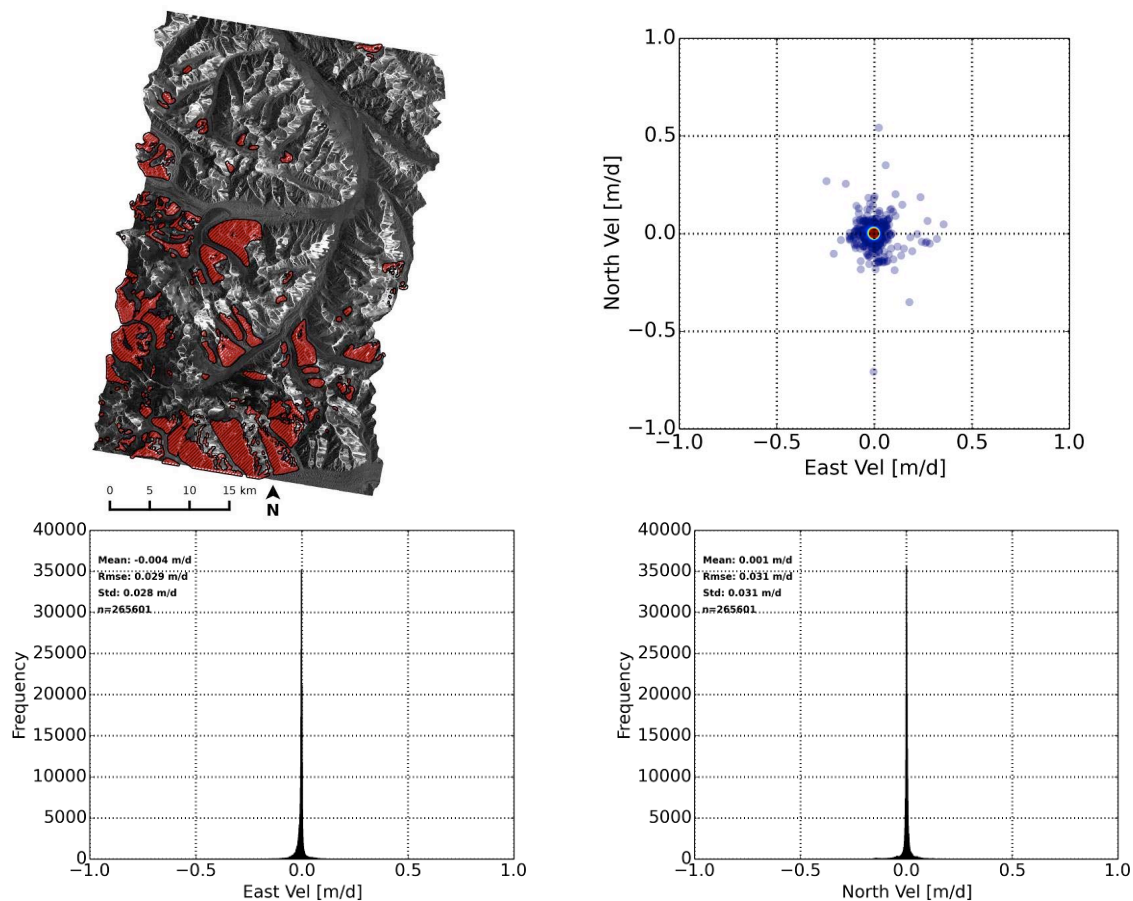


*Figure 6.3: Results of the stable rock test for track 151 (ID: IV-001-05). Upper left panel: stable rock area used in the analysis depicted on the TSX amplitude image. Upper right panel: scatter plot showing easting velocity versus northing velocity with colour coding blue to red indicating point density from low to high. Lower left panel: histogram of easting velocity. Lower right panel: histogram of northing velocity.*
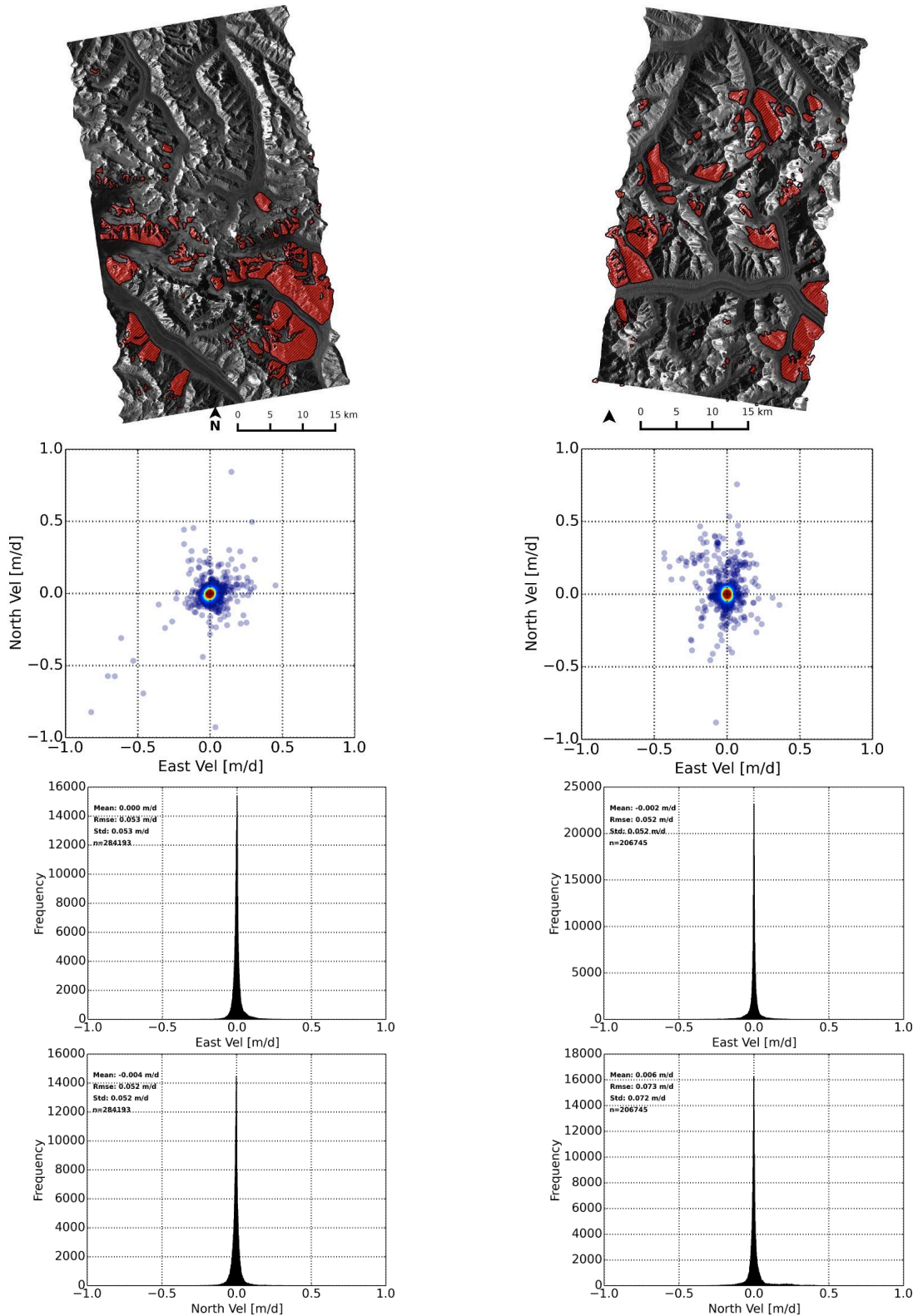
*Figure 6.4: Results of the stable rock test for left track 7 (ID: IV-001-1) and right track 75 (ID: IV-001-02). Upper panel: stable rock area used in the analysis depicted on the TSX amplitude image. Second row from top: scatter plot showing easting velocity versus northing velocity with colour coding blue to red indicating point density from low to high. Third row from top: histogram of easting velocity. Lower panels: histogram of northing velocity.*
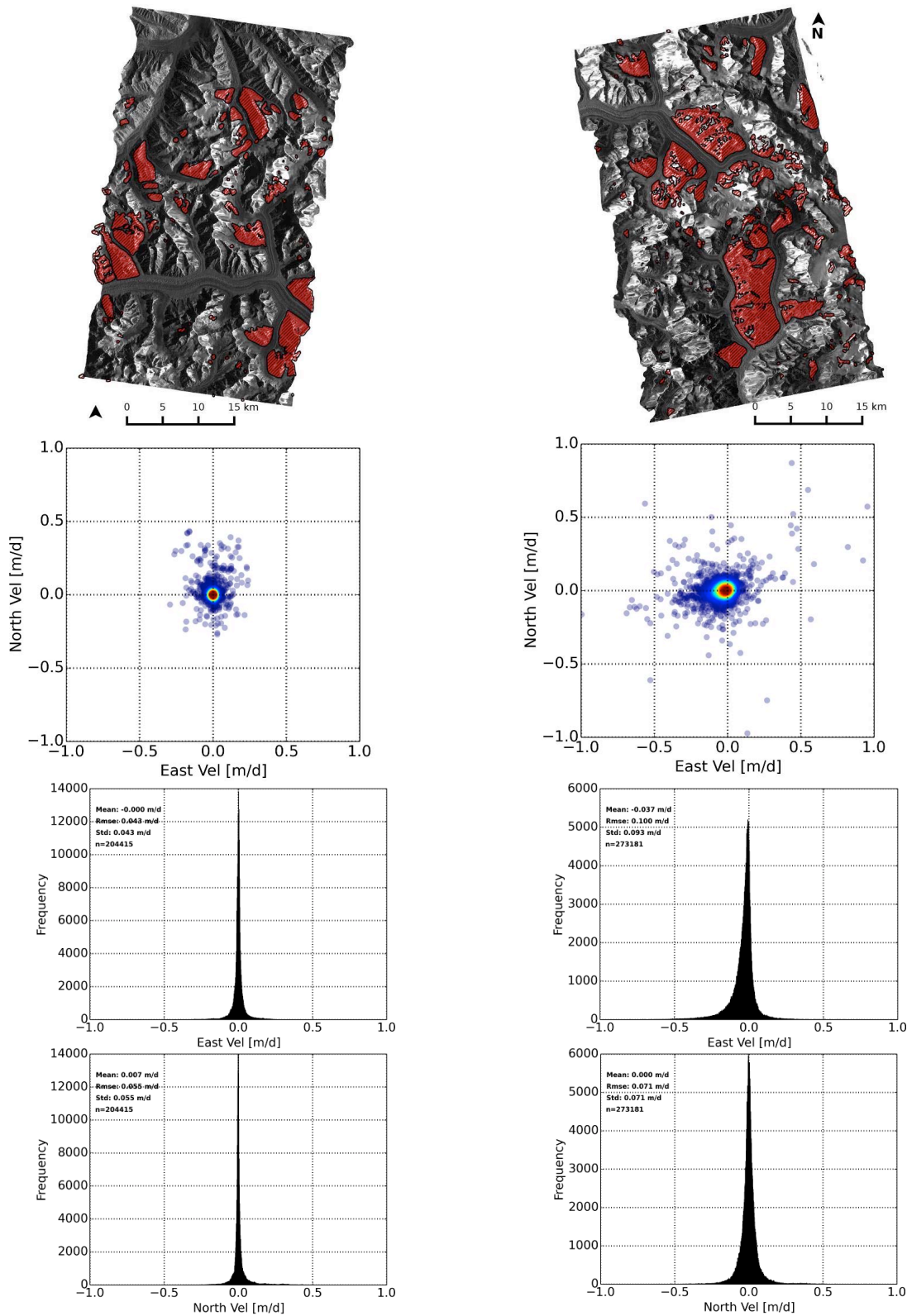
*Figure 6.5: Results of the stable rock test for left track 57 (ID: IV-001-3) and right track 98 (ID: IV-001-04). Upper panel: stable rock area used in the analysis depicted on the TSX amplitude image. Second row from top: scatter plot showing easting velocity versus northing velocity with colour coding blue to red indicating point density from low to high. Third row from top: histogram of easting velocity. Lower panels: histogram of northing velocity.*

## 6.2. Product: Ice Velocity Karakoram PALSAR (ID: IV_rgi14_006)

### 6.2.1. Product description and summary of quality assessment tests

The data sets provide ice velocity of glaciers in the Karakoram region. Ice velocity is derived by SAR offset tracking using ALOS PALSAR image pairs acquired in Fine Beam Single (FBS) mode between 2008 and 2010. The data sets are comprised of compressed ASCII tables (csv format) listing horizontal velocity components (E, N) converted to metres per day (m/d) and signal-to-noise ratio (SNR) coefficients with results in geographic (Lat/Lon) projection. The data products are gridded at 0.00083° (~90 m) and include an xml file (metadata), a quicklook image with a colour scale up to 300 m/yr and a geotiff of the horizontal ice velocities. Table 6.6 is translating the filename to the Product ID in the CRDP. For the data set the quality tests QA-IV-1, QA-IV-2, and QA-IV3 were applied and reported in Table 6.7. Figures 6.6 and 6.7 show examples of the product.

| Filename | Date 1 | Date 2 | Product ID |
|---|---|---|---|
| IV_RGI14_PALSAR_20081211T171949_20090126T172029 | 20081211 | 20090126 | IV-002-1 |
| IV_RGI14_PALSAR_20090102T172900_20090217T172937 | 20090102 | 20090217 | IV-002-2 |
| IV_RGI14_PALSAR_20090114T172445_20090301T172520 | 20090114 | 20090301 | IV-002-3 |
| IV_RGI14_PALSAR_20100127T173944_20100314T173928 | 20100127 | 20100314 | IV-002-4 |

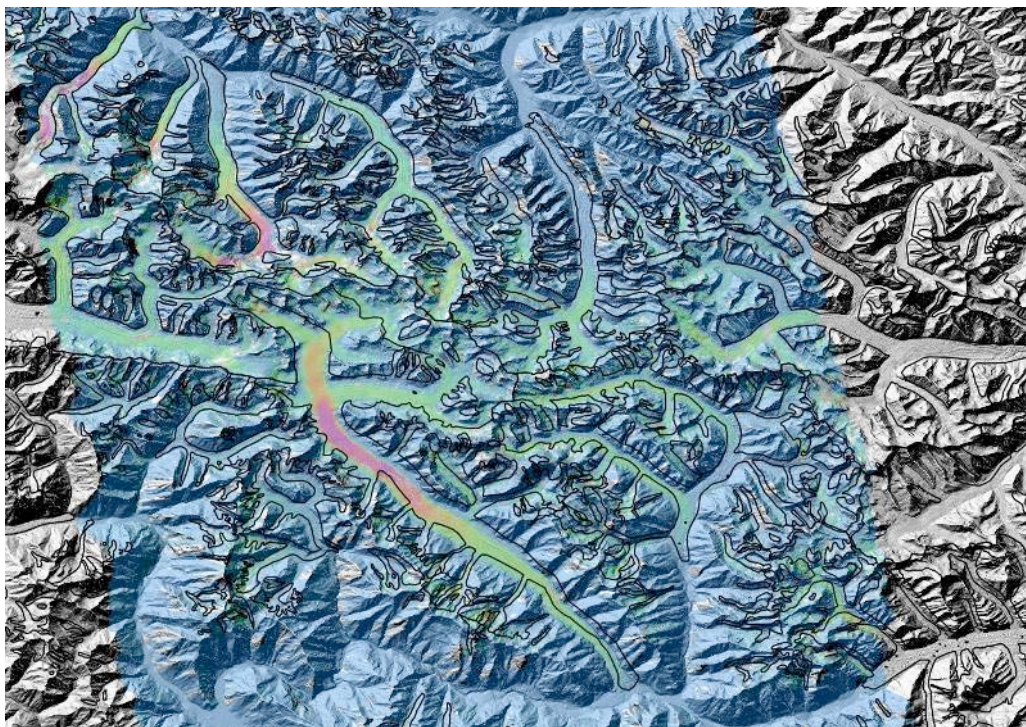*Table 6.6: Overview of filenames and product IDs.*



*Figure 6.6: Ice velocity map for the product IV-002-3 with colour scale up to 300 m/yr. There is a slight shift between RGI 4.0 and the ice velocity map (respectively SRTM v4.1), which results in an apparent higher error characteristic on ice-free regions. The same issue also affects regions where the dates of the glacier outlines and of the ice velocity product are not coincident and there are changes in the glacierized area because of glacier retreat or surges.*

**glaciers cci**

Contract: 4000109873/14/I-NB
Product Validation and Inter-
comparison Report (PVIR)

Name: Glaciers_cci-D4.1_PVIR
Version: 1.6
Date: 21.12. 2017
Page: 32

| Product ID in CRDP | QA-IV-1 [CC/SNR] | QA-IV-2 [% cover] | QA-IV-3 [RMSE in m/day] | | QA-IV-4 | QA-IV-5 |
|---|---|---|---|---|---|---|
| | | | Mean | STD | | |
| IV-002-1 | SNR | 91% | 0.0129976 | 0.0372949 | N/A | N/A |
| IV-002-2 | SNR | 85% | 0.0110903 | 0.0395137 | N/A | N/A |
| IV-002-3 | SNR | 91% | 0.0128416 | 0.0314931 | N/A | N/A |
| IV-002-4 | SNR | 55% | 0.0561153 | 0.0422738 | N/A | N/A |

*Table 6.7: Summary of quality assessment of IV products. QA-IV-2 is related to the % coverage of glacier area for example threshold (STD: standard deviation, N/A: this test was not applied to the data set.*
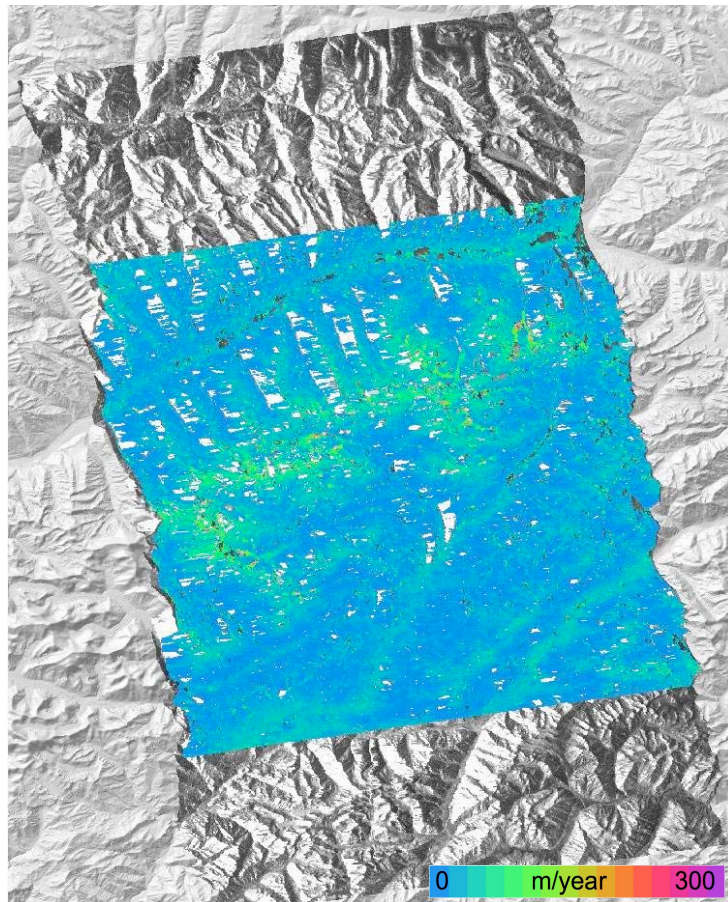


*Figure 6.7: Ice velocity map for product IV-002-4 with colour scale up to 300 m/yr. The coverage of the slave image is smaller than that of the master image (shown as backscattering intensity image) because of data distribution issues, resulting in an apparent low coverage of glacier area of 55%. The automatic tracking procedures implemented in Glaciers_cci considers the coverage of the master image as reference.*

Contract: 4000109873/14/I-NB

**Product Validation and Inter-comparison Report (PVIR)**

Name: Glaciers_cci-D4.1_PVIR
Version: 1.6
Date: 21.12. 2017
Page: 33

## 6.3. Product: Ice Velocity Karakoram PALSAR (ID: IV_rgi14_007)

### 6.3.1. Product description and summary of quality assessment tests

The data sets provide ice velocity of glaciers in the Karakoram region. The ice velocity is derived by SAR offset tracking using ALOS PALSAR image pairs acquired in Fine Beam Dual (FBD) mode between 2007 and 2009. The data sets are comprised of compressed ASCII tables (csv format) listing horizontal velocity components (E, N) converted to metres per day (m/d) and signal-to-noise ratio (SNR) coefficients with results in geographic latitude / longitude projection. The data products are gridded at 0.00083° (~90 m) and include an xml file (metadata), a quicklook image with colour scale up to 300 m/yr and a geotiff of the horizontal ice velocities. The results of quality tests QA-IV-2 and QA-IV3 are reported in Table 6.8 (QA-IV-4 and QA-IV-5 were not performed). Figure 6.8 shows an example of the product.

| Filename | QA-IV-2 [coverage] (%) | QA-IV-3 [RMSE in m/day] | |
|---|---|---|---|
| | | Mean | STD |
| IV_20070608T172039_20070724T172035 | 66 | 0.0284428 | 0.066466 |
| IV_20070613T172721_20070729T172716 | 73 | 0.0328984 | 0.206274 |
| IV_20070618T173355_20070918T173340 | 73 | 0.0144065 | 0.043994 |
| IV_20070705T173602_20070820T173556 | 81 | 0.0183942 | 0.039811 |
| IV_20070712T172502_20070827T172454 | 78 | 0.0290825 | 0.225298 |
| IV_20070722T173810_20071022T173745 | 58 | 0.0138661 | 0.040870 |
| IV_20070722T173818_20071022T173753 | 67 | 0.0160780 | 0.076696 |
| IV_20070724T172035_20070908T172025 | 40 | 0.0231917 | 0.059116 |
| IV_20070805T171559_20070920T171549 | 63 | 0.0216604 | 0.100096 |
| IV_20070808T174008_20070923T173957 | 66 | 0.0095518 | 0.020589 |
| IV_20070808T174016_20070923T174005 | 80 | 0.0112670 | 0.023148 |
| IV_20070810T172241_20070925T172229 | 78 | 0.0213958 | 0.213261 |
| IV_20070810T172249_20070925T172238 | 77 | 0.0298954 | 0.179588 |
| IV_20070815T172923_20070930T172910 | 75 | 0.0460739 | 0.331689 |
| IV_20070822T171813_20071007T171759 | 63 | 0.0154811 | 0.056228 |
| IV_20070822T171829_20071007T171815 | 71 | 0.0174980 | 0.092890 |
| IV_20090722T173308_20090906T173321 | 72 | 0.0367624 | 0.214667 |

*Table 6.8: Summary of quality assessment of IV products. The 'IV_RGI14_PALSAR' in the filename has been shortened to 'IV_' in column 1. Test QA-IV-1 is SNR for all datasets. QA-IV-2 is related to the per cent coverage of glacier area for the example threshold. QA-IV-4 and QA-IV-5 are not shown, as they were not applied to the data set (SNR: Signal to Noise Ratio, STD: standard deviation).*
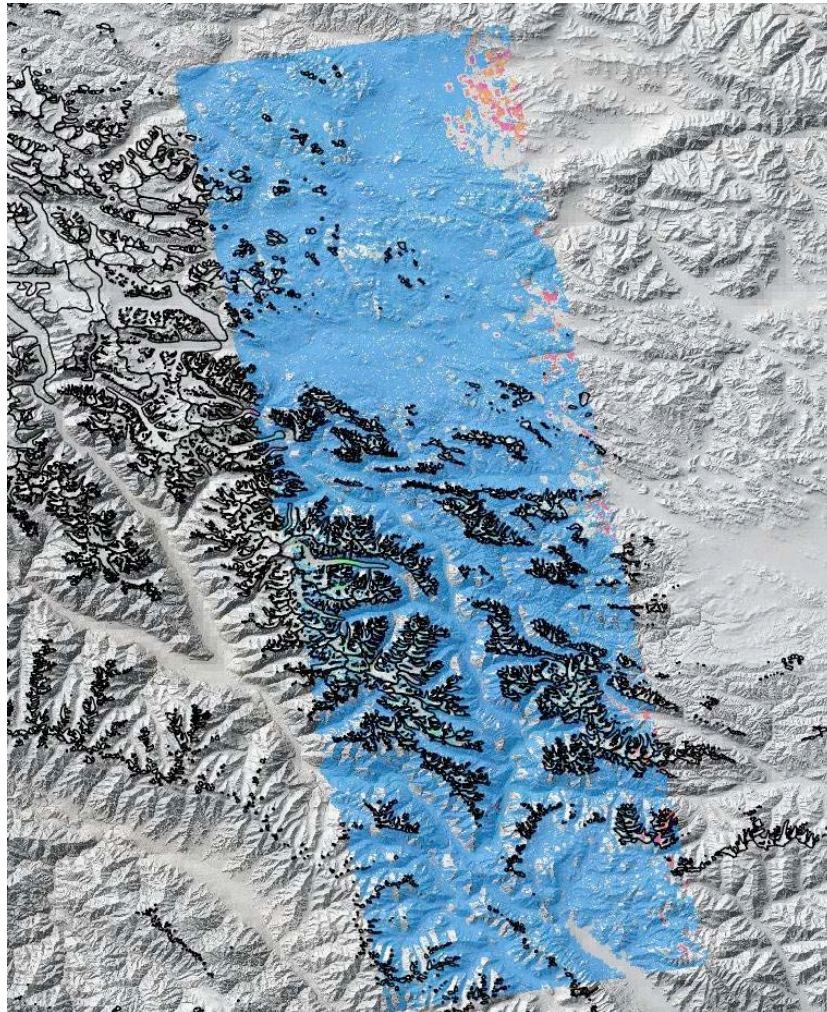
*Figure 6.8: Quicklook of the IV map for dataset IV_20070805T171559_20070920T171549 with a colour scale up to 300 m/yr. There is a large section on the north-east of the image where large, homogeneous offsets were estimated and not successfully removed neither with the SNR coefficient nor with a spatial filter. Because these outliers are outside the glaciers, stronger filters were not applied. This results in a high error characteristic on ice-free regions that might not be representative for the glacier regions.*


## 6.4. Product: Ice Velocity Svalbard Sentinel-1 (ID: IV_rgi07_001)

### 6.4.1. Product description and summary of quality assessment tests

The data sets provide ice velocity of glaciers in the Svalbard Archipelago. The ice velocity is derived by SAR offset tracking using Sentinel-1 image pairs acquired in the Interferometric Wide Swath (IWS) mode in January and February 2015. The data sets are comprised of compressed ASCII tables (csv format) listing velocity components (E, N and vertical) converted to metres per day (m/d) and signal-to-noise ratio (SNR) coefficients with results in UTM zone 33N projection. The data products are gridded at 100 m and include an xml file (metadata), a quicklook image with a colour scale up to 300 m/yr and a geotiff of the horizontal ice velocities. For the data package (Product ID: IV_rgi07_001 in the CRDP) the quality tests QA-IV-1, QA-IV-2, and QA-IV3 were applied and reported in Table 6.9. Figure 6.9 shows an example of the product for the period from January 21 to February 3, 2015.
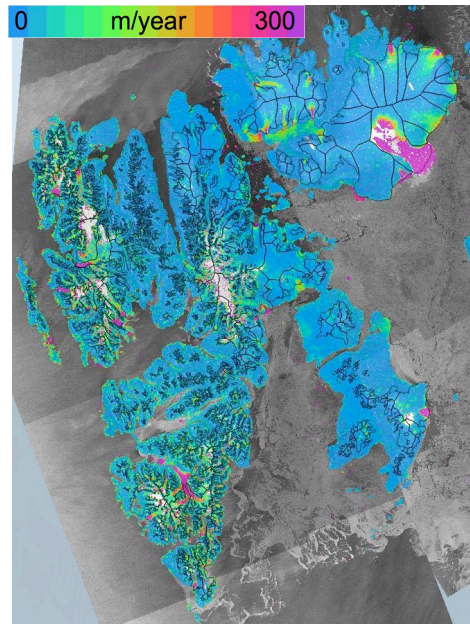
**glaciers cci**

Contract: 4000109873/14/I-NB

**Product Validation and Inter-comparison Report (PVIR)**

Name: Glaciers_cci-D4.1_PVIR
Version: 1.6
Date: 21.12. 2017
Page: 35

*Figure 6.9: Ice velocity map for the product iv_rgi07_001 (time period January 21 to February 3, 2015) over the Svalbard Archipelago with colour scale up to 300 m/yr.*

| Filename | QA-IV-1 [CC/SNR] | QA-IV-2 [% cover] | QA-IV-3 [RMSE in m/day] | |
|---|---|---|---|---|
| | | | **Mean** | **STD** |
| IV_RGI07_S1_20150119T053348_20150131T053348 | SNR | 82 | 0.0837725 | 0.567903 |
| IV_RGI07_S1_20150119T053413_20150131T053413 | SNR | 83 | 0.0212233 | 0.108347 |
| IV_RGI07_S1_20150120T061437_20150201T061437 | SNR | 86 | 0.0349091 | 0.121153 |
| IV_RGI07_S1_20150120T061502_20150201T061502 | SNR | 85 | 0.0616598 | 0.229044 |
| IV_RGI07_S1_20150120T061527_20150201T061527 | SNR | 78 | 0.0951199 | 0.180285 |
| IV_RGI07_S1_20150121T150336_20150202T150336 | SNR | 92 | 0.0218558 | 0.040451 |
| IV_RGI07_S1_20150121T150402_20150202T150402 | SNR | 80 | 0.0355463 | 0.175555 |
| IV_RGI07_S1_20150121T150427_20150202T150427 | SNR | 82 | 0.0198538 | 0.033592 |
| IV_RGI07_S1_20150122T154416_20150203T154416 | SNR | 28 | 0.0778865 | 0.070041 |
| IV_RGI07_S1_20150122T154443_20150203T154443 | SNR | 89 | 0.0819516 | 0.292675 |
| IV_RGI07_S1_20150122T154508_20150203T154508 | SNR | 88 | 0.0569449 | 0.201304 |
| IV_RGI07_S1_20150122T154534_20150203T154534 | SNR | 74 | 0.0389312 | 0.073646 |
| IV_RGI07_S1_20150202T150336_20150214T150336 | SNR | 87 | 0.0257894 | 0.042046 |
| IV_RGI07_S1_20150202T150402_20150214T150401 | SNR | 63 | 0.0430565 | 0.063249 |
| IV_RGI07_S1_20150202T150427_20150214T150426 | SNR | 47 | 0.0392932 | 0.040525 |
| IV_RGI07_S1_20150203T154416_20150215T154415 | SNR | n/a | n/a | n/a |
| IV_RGI07_S1_20150203T154443_20150215T154443 | SNR | 89 | 0.0612753 | 0.136987 |
| IV_RGI07_S1_20150203T154508_20150215T154508 | SNR | 82 | 0.0684827 | 0.089888 |
| IV_RGI07_S1_20150203T154534_20150215T154533 | SNR | 74 | 0.0877673 | 0.115890 |

*Table 6.9: Summary of quality assessment of IV products. QA-IV-2 is related to the per cent coverage of glacier area for example threshold, STD is the standard deviation, QA-IV-4 and QA-IV-5 were not performed for the listed datasets.*

### 6.4.2. Reference validation dataset

No in-situ validation data or validation data from other sensors are available to us for the Svalbard Archipelago for the time period of the IV products generated for the CRDP. Howev-

![glaciers cci logo]

| Contract: 4000109873/14/I-NB | Name: | Glaciers_cci-D4.1_PVIR |

**Product Validation and Inter-comparison Report (PVIR)**

Version: 1.6
Date: 21.12. 2017
Page: 36

er, it was possible in the framework of the EU FP7 SEN3APP project (http://sen3app.fmi.fi) to obtain three Radarsat-2 Wide Ultra Fine Mode acquisitions over Stonebreen on Edgeøya for February 4, February 28 and March 23, 2016. Radarsat-2 (RSAT2) Wide Ultra Fine Mode have a spatial resolution of about 3 m and cover an area of approximately 50 km x 50 km. Thanks to the regular acquisitions of Sentinel-1 data over the Svalbard Archipelago every 12 days along descending orbits, it was possible to perform a intercomparison of Sentinel-1 Interferometric Wide Swath (IWS) data. Sentinel-1 data used for the intercomparison are from February 9 to 21, 2016 and March 4 to 16, 2016, not exactly the same time period of the RSAT2 data but close. Figure 6.10 visualizes the comparison of the Sentinel-1 and Radarsat-2 ice velocity products over Stonebreen. The results for the quality tests QA-IV-1, QA-IV-2, QA-IV3 and QA-IV4 are reported in Table 6.10. Overall, we observe a good match of the Sentinel-1 and Radarsat-2 data over stable terrain, with error estimates on the order of 0.1 m/day (36 m/yr) resp. 0.05 m/day (18 m/yr). The intercomparison between the two data sets indicates values approaching 0.15 m/day (or 50 m/year). Some outliers due to residual noise on the Sentinel-1 data are observed, e.g. at 8 km from the front position. In comparison to the 2015 Sentinel-1 data of the CRDP the coverage of ice surface velocity data over glacier area is much reduced in 2016, because in 2015-2016 the winter was much warmer than in 2014-2015. However, the 2016 validation results should be applicable also for the 2015 products.

| Filename | QA-IV-1 [CC/SNR] | QA-IV-2 [% cover] | QA-IV-3 [RMSE in m/day] | | QA-IV-4 | QA-IV-5 [RMSE in m/day] | |
|---|---|---|---|---|---|---|---|
| | | | Mean | STD | | Mean | STD |
| IV_RGI07_S1_20160209T150337_20160221T150337 | CC | 43 | 0.06595 | 0.117847 | N/A | –0.02543 | 0.14636 |
| IV_RGI07_S1_20160304T150338_20160316T150338 | CC | 34 | 0.021223 | 0.108347 | N/A | –0.00416 | 0.15046 |
| IV_RGI07_RSAT2_20160204T150954_20160228T150953 | CC | 47 | 0.014643 | 0.046237 | N/A | N/A | N/A |
| IV_RGI07_RSAT2_20160228T150953_20160323T20160228T150952 | CC | 37 | 0.039137 | 0.072819 | N/A | N/A | N/A |

*Table 6.9: Summary of quality assessment of IV products. QA-IV-2 is related to the per cent coverage of glacier area for example threshold, STD is standard deviation, for N/A this test was not applied to the data set.*
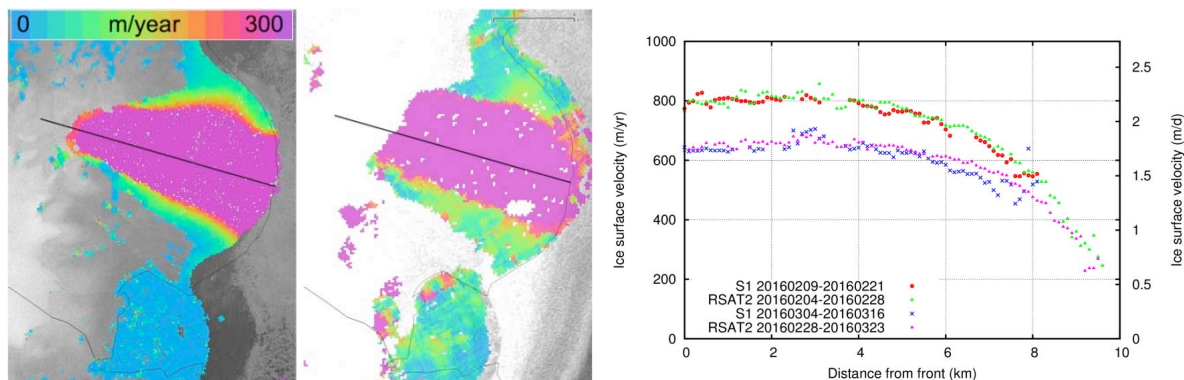


*Figure 6.10: Sentinel-1 Interferometric Wide Swath 2016.03.04-2016.03.17 (left), Radarsat-2 Wide Ultra Fine Mode 2016.02.28_2016.03.23 (middle), and comparison along the centre line of Stonebreen (right) shown as a black line on the Sentinel-1 and Radarsat-2 maps.*

## 6.5. Product: Ice Velocity South Georgia (ID: IV_rgi19_002/003 )

Ice velocity for glaciers in South Georgia is derived by SAR offset tracking using ALOS PALSAR image pairs acquired in Fine Beam Dual polarization (FBD) mode between May and July 2010 (IV_rgi19_003) and TSX image pairs acquired on 25.06.2013 and 28.07.2013 (IV_rgi19_002). The offset tracking algorithm performs iterative template matching with a variable window size to allow shearing zones and spatial variation of glacier velocity to be resolved better. Post processing steps include basic filtering to exclude outliers and masking areas affected by layover. The final product is clipped using an ocean mask based on a DEM. The data sets are comprised of compressed ASCII tables (csv format) as specified in the PSD listing the three velocity components (easting, northing and vertical) in metres per day (m d$^{-1}$) and correlation coefficients with results in UTM 24S projection. The vertical velocity is derived from the interpolated height difference of the end position of the displacement vector and the start position, taken from the ASTER Global Digital Elevation Model V2 (USGS, 2015). The data products are posted at 50 m and include an xml file (metadata) and a quick-look image. Figure 6.11 shows the magnitude of the horizontal velocity derived from PAL-SAR and TSX depicted on a PALSAR amplitude image, velocities reach up to 3 m/d on the larger outlet glaciers.
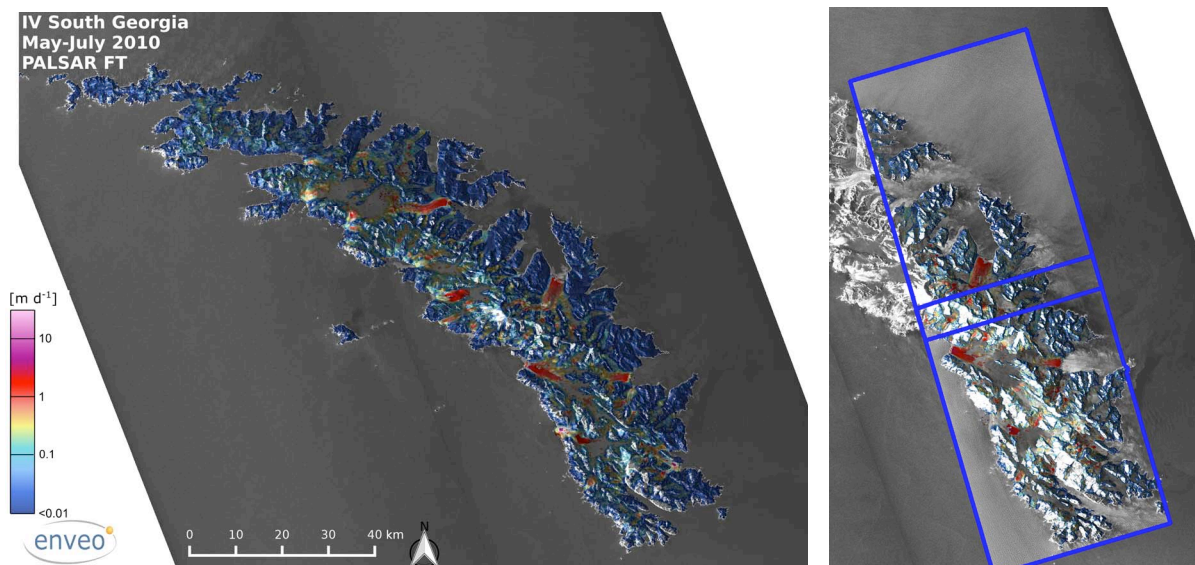


*Figure 6.11: Magnitude of ice velocity on South Georgia derived from: (left) ALOS PALSAR image pairs acquired between May and July 2010, and (right) TSX image pairs acquired on 25.06.2013 and 28.07.2013. Background: PALSAR amplitude image, blue outlined area shows extend of TSX image pairs.*

### 6.5.1. QA-IV-2: Coverage of IV measurements

Figure 6.12 and Table 6.11 give an overview of the total glacierized area and the coverage of successful IV measurements for each product. Calculation of glacier area is based on the RGI 5.0 (Pfeffer et al., 2014) with outlines for this region provided by Glaciers_cci. The iterative processing provides good coverage of the glaciers and resolves shearing zones and spatial variation of the velocity. There are some gaps on the slower inland glaciers where there are less features and in some of the shearing zones on the faster glaciers.
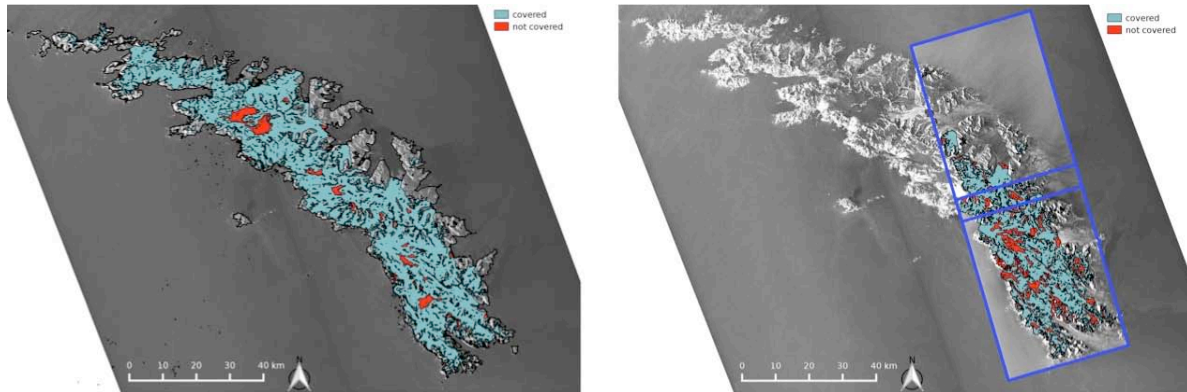
*Figure 6.12: Outline of glacierized terrain in South Georgia based on RGI 5.0 (Pfeffer et al., 2014) and indication of IV coverage (cyan: covered, red: not covered) derived from: (left) ALOS PALSAR image pairs acquired between May and July 2010, and (right) TSX image pairs acquired on 25.06.2013 and 28.07.2013. Background: PALSAR amplitude image, blue outlined area shows extend of TSX image pairs.*

| Sensor/Track | Glacier area [km$^2$] | IV area [km$^2$] | Coverage [%] |
|---|---|---|---|
| PALSAR/66 | 2350 | 2165 | 92.1 |
| PALSAR/67 | 2922 | 2624 | 89.8 |
| PALSAR/68 | 1189 | 1075 | 90.4 |
| TSX/42a | 1245 | 981 | 78.8 |
| TSX/42b | 348 | 296 | 85.0 |

*Table 6.11: Total glacier area, IV area and percentage coverage for IV products.*

### 6.5.2.  QA-IV-3: Stable Rock analysis of IV products

No in-situ validation data or validation data from other sensors are available for the region and time period of the generated IV products. An alternative approach for quality assessment of the velocity products is the analysis of stable ground i.e. where no velocity is expected. This gives an overall indication for the bias introduced by the velocity retrieval including co-registration of images, etc. After performing the matching for the entire region covered by the image pairs, the results for ice covered (moving) terrain is separated from ice-free (stable) terrain (Figure 6.13). The masking is done using a polygon of glacier outlines based on RGI 5.0 (Pfeffer et al., 2014). Buffers around the glacier polygon are applied before extraction of stable ground for statistics calculation. The analysis has been performed for both easting and northing velocity components. The quality metrics of the test provide mean and RMSE of the velocity over stable terrain; ideally mean values should be close to 0. Results show that both the northing and easting velocity components are scattered around a zero mean indicating no bias, and with a low RMSE of 2 to 4 cm/d for PALSAR and 8 to 10 cm/d for TSX (Table 6.12). The larger RMSE values for TSX are possibly related to differences in algorithm settings, aerial coverage and time interval.

glaciers
cci

Contract: 4000109873/14/I-NB
Product Validation and Inter-
comparison Report (PVIR)

Name: Glaciers_cci-D4.1_PVIR
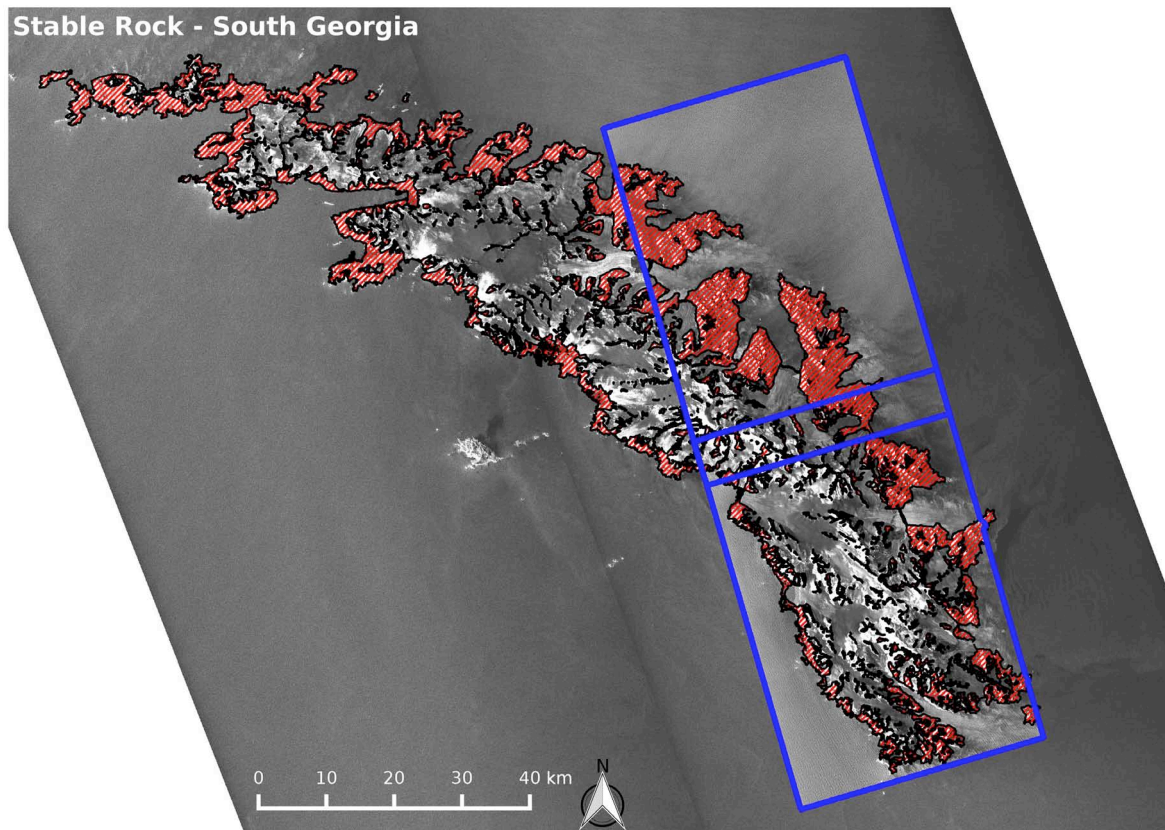Version: 1.6
Date: 21.12. 2017
Page: 39

*Figure 6.13: Stable rock area in South Georgia based on RGI 5.0 (Pfeffer et al., 2014) and used for the stable rock analysis. Background: PALSAR amplitude image, blue outlined area shows extend of TSX image pairs.*

| Track | Number of pixels | Mean E [m d⁻¹] | RMSE E [m d⁻¹] | Mean N [m d⁻¹] | RMSE N [m d⁻¹] |
|---|---|---|---|---|---|
| 66 | 306,149 | 0.00 | 0.03 | 0.00 | 0.02 |
| 67 | 339,049 | 0.00 | 0.04 | 0.00 | 0.03 |
| 68 | 145,754 | 0.00 | 0.04 | 0.00 | 0.03 |
| TSX/42a | 86560 | 0.00 | 0.09 | 0.00 | 0.08 |
| TSX/42b | 97881 | 0.03 | 0.10 | 0.00 | 0.08 |

*Table 6.12: Summary of stable rock quality assessment for PALSAR and TSX derived velocities on South Georgia.*

## 6.6.  Product: Ice Velocity Alexander Island, Antarctica (ID: IV_rgi19_004)

The IV data set provides ice velocity of glaciers on Alexander Island, Antarctica. Ice velocity is derived by SAR offset tracking using Sentinel-1 image pairs acquired in Interferometric Wide Swath (IW) mode and is averaged over the period October 2014 - February 2016. Post processing steps include basic filtering to exclude outliers and masking out areas affected by layover. The final product is clipped using an outline shapefile of the island from RGI 5.0 (Pfeffer et al., 2014). The data set is comprised of compressed ASCII tables (csv format) as specified in the PSD listing the three velocity components (easting, northing and vertical) in metres per day (m d$^{-1}$). The vertical velocity is derived from the interpolated height difference of the end position of the displacement vector and the start position, taken from the Radarsat Antarctic Mapping Project Digital Elevation Model, Version 2 (Liu et al., 2001). This 200m DEM provides the best quality for Antarctica and has little artefacts. The data products are posted at 200 m in Antarctic Polar Stereographic projection and include an xml file (metadata) and a quicklook image.

### 6.6.1.  QA-IV-2: Coverage of IV measurements

Figure 6.14 and Table 6.13 give an overview of the total glacierized area and the coverage of successful IV measurements for the product. Calculation of glacier area is based on the RGI 5.0 (Pfeffer et al., 2014) with outlines for this region provided by Glaciers_cci. Overall more than 96% of the island is covered by IV measurements.
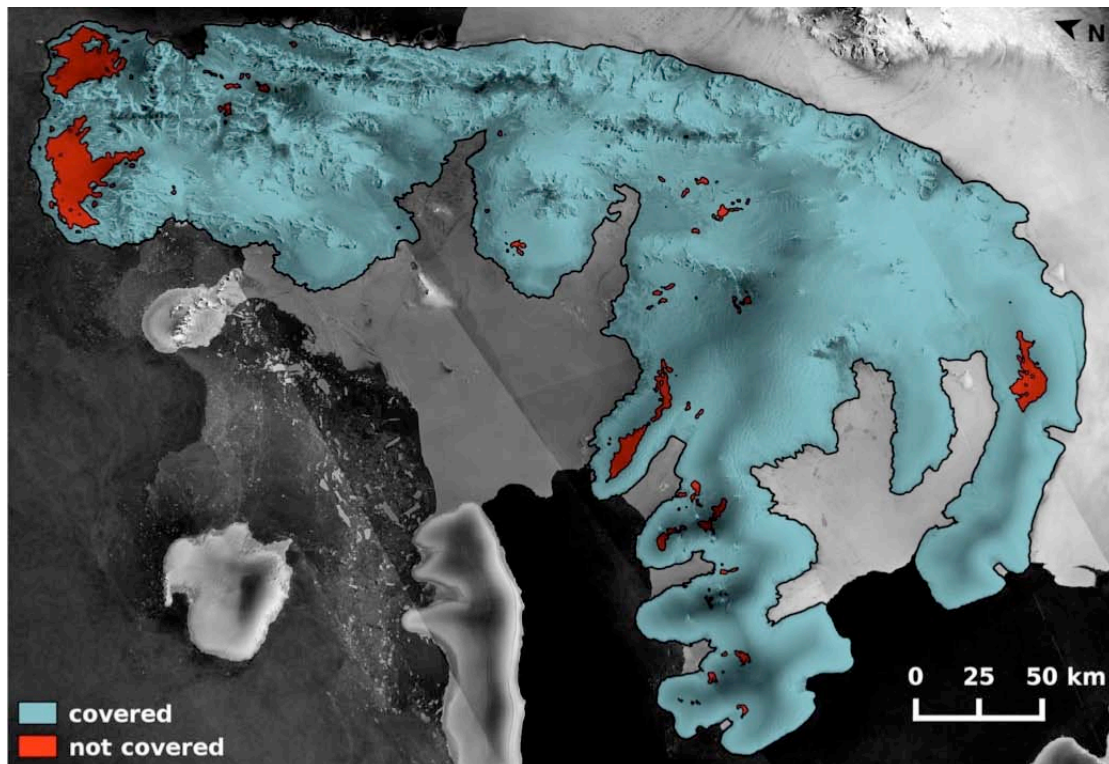


*Figure 6.14: Outline of Alexander Island, Antarctica based on RGI 5.0 (Pfeffer et al., 2014) and indication of IV coverage (cyan: covered, red: not covered) derived from Sentinel-1 acquired between 2014-2016 (background: Sentinel-1 amplitude mosaic).*

![glaciers cci logo]

Contract: 4000109873/14/I-NB
**Product Validation and Inter-comparison Report (PVIR)**

Name:     Glaciers_cci-D4.1_PVIR
Version:  1.6
Date:     21.12. 2017
Page:     41

| Sensor/Product ID | Glacier area [km$^2$] | IV area [km$^2$] | Coverage [%] |
|---|---|---|---|
| Sentinel-1/IV_rgi19_004 | 48,806 | 46,929 | 96.2 |

*Table 6.13: Total glacier area, IV area and percentage coverage for the Sentinel-1 IV product covering Alexander Island.*

### 6.6.2.  QA-IV-3: Stable Rock analysis of IV product

The ice covered (moving) terrain is separated from ice-free (stable) terrain (Figure 6.15). The masking is done using a polygon of glacier outlines based on RGI 5.0. Buffers around the glacier polygon are applied before extraction of stable ground for statistics calculation. The analysis has been performed for both easting and northing velocity components. The quality metrics of the test provide mean and RMSE of the velocity over stable terrain. Results show that both the northing and easting velocity components are scattered around a zero mean indicating no bias, and with a low RMSE of 3 cm/d (Table 6.14).
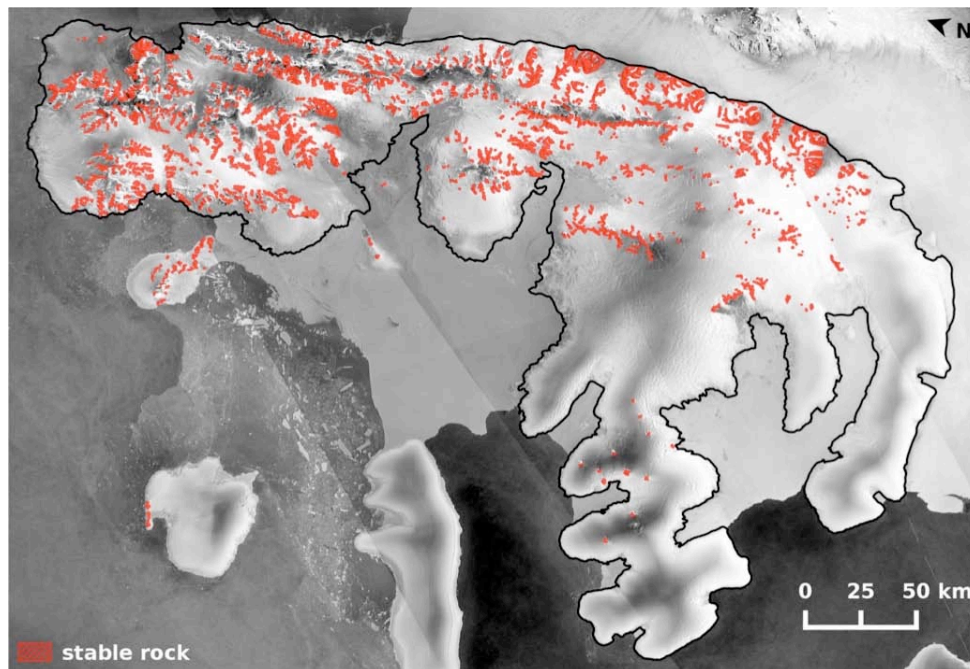


*Figure 6.15: Stable rock area in Alexander Island, Antarctica, based on RGI 5.0 and used for the stable rock analysis (background: Sentinel-1 amplitude mosaic).*

| Sensor/Product ID | Number of pixels | Mean E [m d$^{-1}$] | RMSE E [m d$^{-1}$] | Mean N [m d$^{-1}$] | RMSE N [m d$^{-1}$] |
|---|---|---|---|---|---|
| Sentinel-1 /IV_rgi19_004 | 3418 | 0.00 | 0.03 | 0.00 | 0.03 |

*Table 6.14: Summary of stable rock quality assessment for Sentinel-1 derived velocities on Alexander Island.*

### 6.6.3.  QA-IV-5: Inter-comparison of Sentinel-1 with Measures IV product

No in-situ validation data or validation data from other sensors are available for the region and time period of the generated IV products. Here we make a comparison with data from the MEaSUREs project (Rignot et al., 2011) (Figure 6.16).
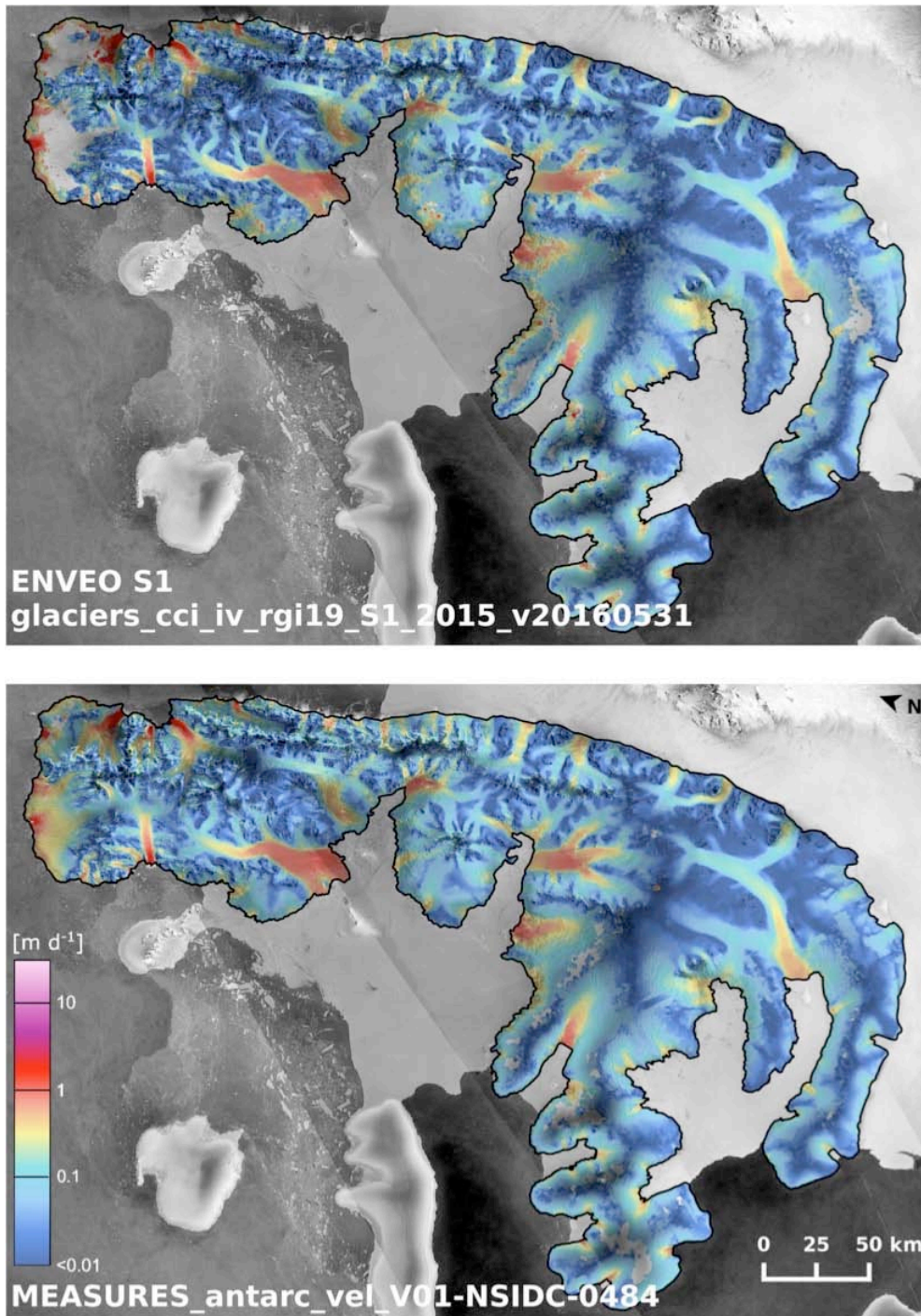
Contract: 4000109873/14/I-NB
Product Validation and Inter-
comparison Report (PVIR)

Name:     Glaciers_cci-D4.1_PVIR
Version:  1.6
Date:     21.12. 2017
Page:     42



*Figure 6.16: IV map of Alexander Island from Sentinel-1 (top) and MEaSUREs (bottom). Background: Sentinel-1 amplitude mosaic.*

The MEaSUREs ice velocity map of Antarctica is a composite product derived from different sources (including ERS, ENVISAT, PALSAR, RADARSAT) and covering a wide temporal range (primarily IPY, 2007-2009, but with patches filled in with data from 1996 and 2000). Therefore, the inter-comparison should not be viewed as a validation, but it can nevertheless provide useful information on data quality and a possible bias is easily identified in particular for regions where not much change is expected such as slow moving interior ice. Before the

glaciers cci

Contract: 4000109873/14/I-NB
Product Validation and Inter-comparison Report (PVIR)

Name:       Glaciers_cci-D4.1_PVIR
Version:    1.6
Date:       21.12. 2017
Page:       43

inter-comparison the Sentinel-1 derived IV map was resampled to the same grid spacing of the Measures IV map (450 m). The latter was then subtracted from the Sentinel-1 map for both the easting and northing components of velocity separately; a difference plot is also produced for velocity magnitude (Figure 6.17). Results show that both the northing and easting velocity residuals are scattered around a zero mean indicating no bias, and with a RMSE of 6 to 7 cm/d (Table 6.15 and Figure 6.17). The difference map indicates little change for the majority of the island but also indicates some areas/glaciers with larger differences both positive and negative. It needs to be further investigated whether they are artefacts of the filtering or gridding or represent real change.
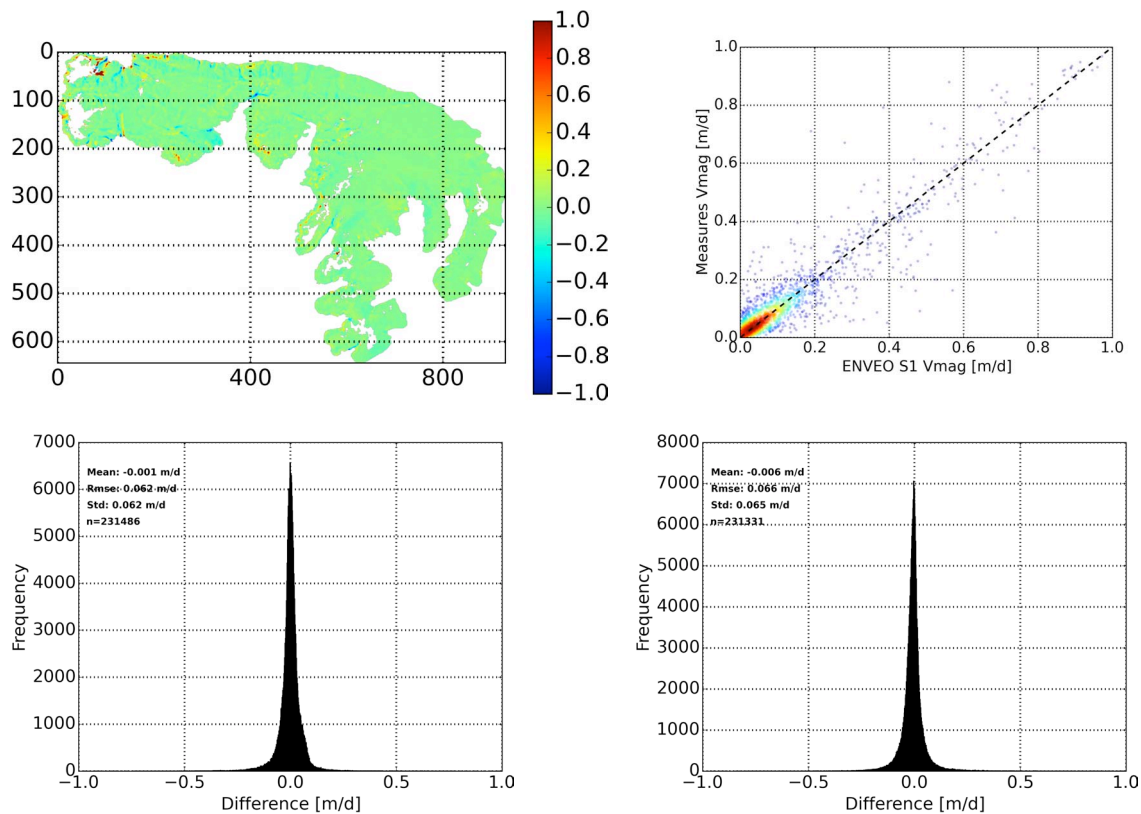


*Figure 6.17: Results of the inter-comparison between Sentinel-1 derived IV map of Alexander Island and the MEaSUREs IV map. Upper left: difference map of velocity magnitude (Sentinel-1 minus MEaSUREs), negative values mean higher IV from MEaSUREs and vice versa. Upper right: scatter plot for velocity magnitude with colour coding blue to red indicating increasing point density and dashed line representing unity. Lower left: histogram of easting velocity difference. Lower right: histogram of northing velocity difference.*

| Number of pixels | Mean difference Easting [m d⁻¹] | RMSE E difference [m d⁻¹] | Mean difference Northing [m d⁻¹] | RMSE N difference [m d⁻¹] |
|---|---|---|---|---|
| 231,486 | 0.00 | 0.06 | -0.01 | 0.07 |

*Table 6.15: Summary of differences between Sentinel-1 derived IV map of Alexander Island and the MEaSUREs IV map.*

## 6.7. Product: Ice Velocity Alexander Island, Antarctica (ID: IV_rgi19_005)

The IV data set provides an ice velocity mosaic of glaciers on Alexander Island, Antarctica. Ice velocity is derived by SAR offset tracking using ALOS PALSAR image pairs acquired in Fine Beam Single (FBS) mode in the period Aug-Dec 2010. Post processing steps include basic filtering to exclude outliers and masking out areas affected by layover. The final product is clipped using an outline shapefile of the island from RGI 5.0 (Pfeffer et al., 2014). The data set is comprised of a compressed ASCII table (csv format) as specified in the PSD listing the three velocity components (easting, northing and vertical) in metres per day (m d$^{-1}$) as well as in (3-layer) GeoTiff format. The vertical velocity is derived from the interpolated height difference of the end position of the displacement vector and the start position, taken from the Radarsat Antarctic Mapping Project Digital Elevation Model, Version 2 (Liu et al., 2001). This 200m DEM provides the best quality for Antarctica and has little artefacts. The IV product is posted at 200 m in Antarctic Polar Stereographic projection and includes an xml file (metadata) and a quicklook image. For the data set the quality tests QA-IV-2, QA-IV-3, and QA-IV-5 were applied. Figure 6.18 shows a quicklook of the velocity magnitude.
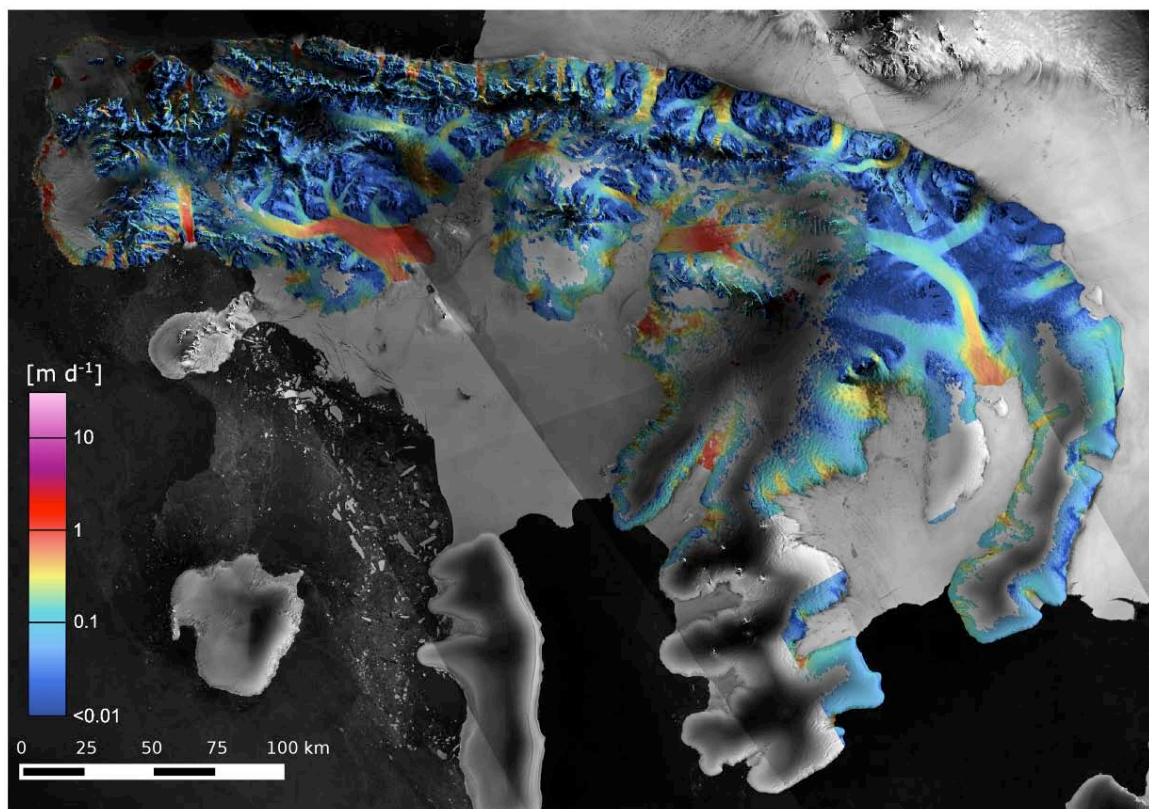


*Figure 6.18: IV map of Alexander Island from ALOS PALSAR data acquired in 2010. Background: Sentinel-1 amplitude mosaic.*

### 6.7.1. QA-IV-2: Coverage of IV measurements

Figure 6. and Table 6.106 give an overview of the total glacierized area and the coverage of successful IV measurements of the product. Calculation of glacier area is based on the RGI 5.0 (Pfeffer et al., 2014) with outlines for this region provided by Glaciers_cci. Overall about 72% of the island is covered by the IV measurements.

![glaciers cci logo]

Contract: 4000109873/14/I-NB

Product Validation and Inter-
comparison Report (PVIR)

Name:     Glaciers_cci-D4.1_PVIR
Version:  1.6
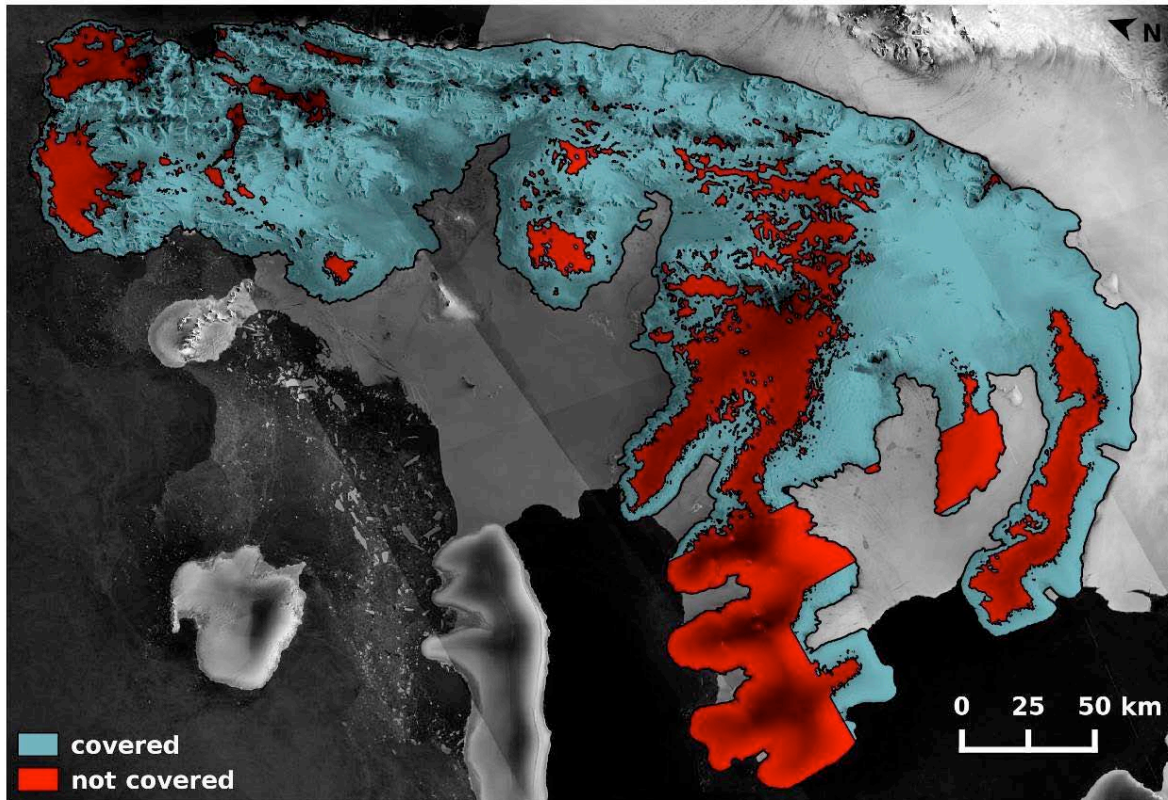Date:     21.12. 2017
Page:     45

*Figure 6.19: Outline of Alexander Island, Antarctica based on RGI 5.0 (Pfeffer et al., 2014) and indication of IV coverage (cyan: covered, red: not covered) derived from ALOS PALSAR acquired in 2010 (background: Sentinel-1 amplitude mosaic).*

| Sensor/Product ID | Glacier area [km$^2$] | IV area [km$^2$] | Coverage [%] |
|---|---|---|---|
| PALSAR/IV_rgi19_005 | 48,806 | 34,942 | 71.6 |

*Table 6.106: Total glacier area, IV area and percentage coverage for the ALOS PALSAR IV product covering Alexander Island.*

### 6.7.2. QA-IV-3: Stable rock analysis of IV product

The ice covered (moving) terrain is separated from ice-free (stable) terrain (Figure 6.15). The masking is done using a polygon of glacier outlines based on RGI 5.0. Buffers around the glacier polygon are applied before extraction of stable ground for statistics calculation. The analysis has been performed for both easting and northing velocity components. The quality metrics of the test provide mean and RMSE of the velocity over stable terrain. Results show that both the northing and easting velocity components are scattered around a zero-mean indicating no bias, and with a low RMSE of 3 cm/d (7).

| Sensor/Product ID | Number of pixels | Mean E [m d$^{-1}$] | RMSE E [m d$^{-1}$] | Mean N [m d$^{-1}$] | RMSE N [m d$^{-1}$] |
|---|---|---|---|---|---|
| PALSAR/IV_rgi19_005 | 11,369 | 0.01 | 0.03 | 0.00 | 0.03 |

*Table 6.117: Summary of stable rock quality assessment for ALOS PALSAR derived velocities on Alexander Island.*

### 6.7.3.  QA-IV-5: Inter-comparison of ALOS PALSAR with Sentinel-1 & Measures IV product

Here we make a comparison with the IV mosaic of Alexander Island acquired from Sentinel-1 (IV_rgi19_004) as well as from the MEaSUREs project (Rignot et al., 2011) (see Section 6.6 and Figure 6.16). The Sentinel-1 IV product is provided at the same grid spacing and the quality test does therefore not require a resampling of the data. The Sentinel-1 mosaic is averaged over the period October 2014 - February 2016, so there is a temporal difference of about 6 years. In contrast, the MEaSUREs mosaic is provided at 450 m grid spacing and therefore requires resampling of the ALSO PALSAR data set (also to 450 m), while there is not a clear time stamp for the product and the source data covers more than a decade (see Section 6.6.3). Results show for both data sets and for both the northing and easting velocity components that residuals are scattered around a zero-mean indicating little change and no bias, and with a low RMSE of 7 cm/d to 9 cm/d (Table 6.128). The difference maps show minor differences for most of the island but also indicates some areas/glaciers with larger differences both positive and negative (Figure 6.20). It needs to be further investigated whether they are artefacts of the filtering or gridding or represent real change.

| Product | Number of pixels | Mean difference Easting [m d$^{-1}$] | RMSE E difference [m d$^{-1}$] | Mean difference Northing [m d$^{-1}$] | RMSE N difference [m d$^{-1}$] |
| --- | --- | --- | --- | --- | --- |
| IV_rgi19_004 | 870,581 | 0.01 | 0.09 | 0.00 | 0.08 |
| MEaSUREs | 178,464 | 0.00 | 0.08 | -0.01 | 0.07 |

*Table 6.128: Summary of differences between ALSO PALSAR derived IV map of Alexander Island versus Sentinel-1 (IV_rgi19_004) and MEaSUREs.*
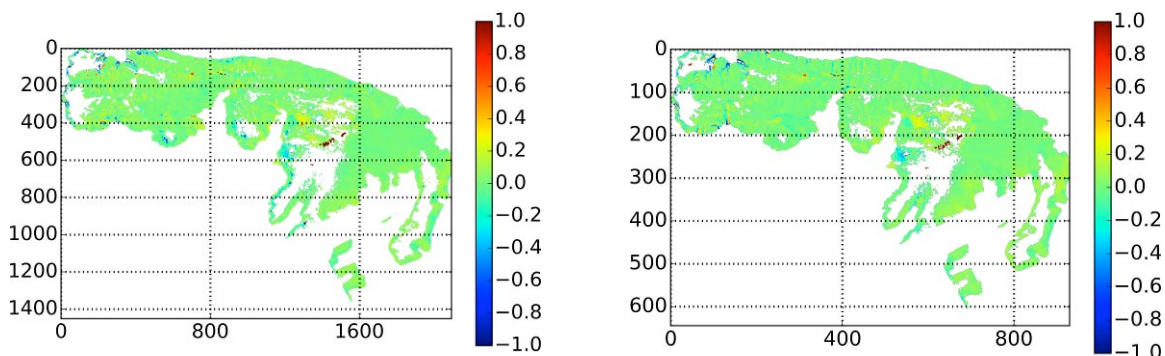


*Figure 6.20: Difference map of IV (in m/d) derived by ALOS PALSAR and Sentinel-1 (left) and MEaSUREs (right).*

## 6.8. Product: Ice Velocity South Georgia (ID: IV_rgi19_006)

The IV data set provides a velocity mosaic of glaciers on South Georgia. Ice velocity is derived by SAR offset tracking using Sentinel-1 image pairs acquired in Interferometric Wide Swath (IW) mode and is averaged over the period July 2016 to October 2016. The final product is clipped using an ocean mask based on a DEM threshold. The data set is comprised of a compressed ASCII table (csv format) as specified in the PSD, listing the three velocity components (easting, northing and vertical) in metres per day (m d$^{-1}$) in UTM 24S projection as well as in (3-layer) GeoTiff format. The vertical velocity is derived from the interpolated height difference of the end position of the displacement vector and the start position, taken from the ASTER GDEM V2 (USGS, 2015). The data product is posted at 200 m and includes an xml file (metadata) and a quicklook image. Figure 6.2121 shows the magnitude of the horizontal velocity depicted on a Sentinel-1 amplitude image. No in-situ validation data or validation data from other sensors are available for the region and time period of the generated IV products. For the data set the quality tests QA-IV-2, QA-IV-3 were applied.
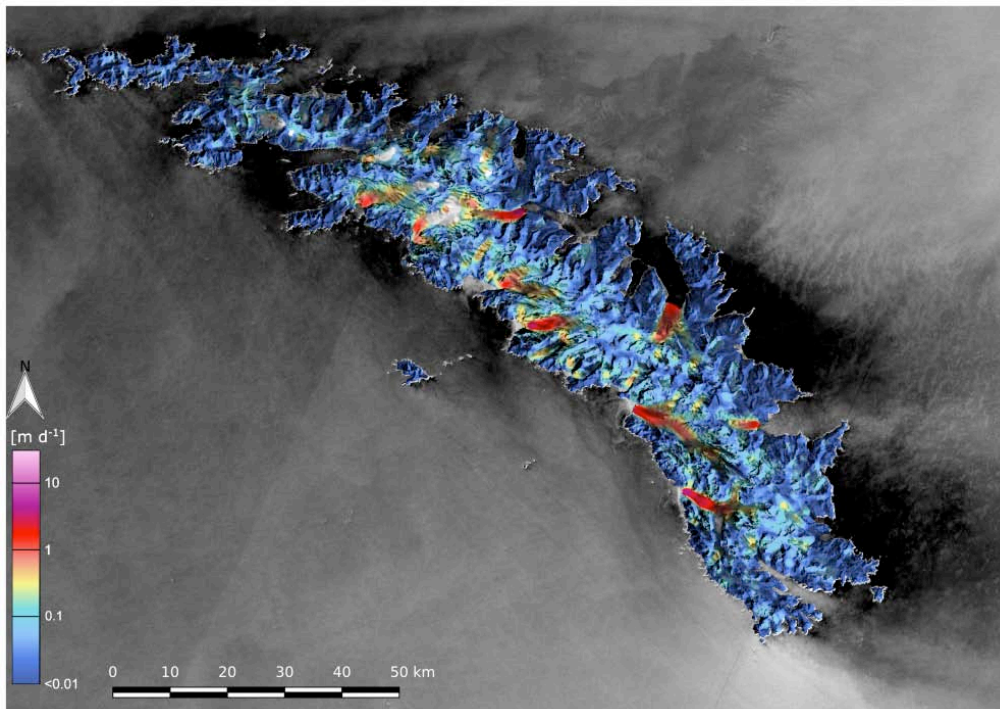


*Figure 6.21: IV map of South Georgia from Sentinel-1 data acquired in 2016. Background: Sentinel-1 amplitude mosaic.*

### 6.8.1. QA-IV-2: Coverage of IV measurements

Figure 6.22 and Table 6.13: Total glacier area, IV area and percentage coverage for the Sentinel-1 IV product covering South Georgia. give an overview of the total glacierized area and the coverage of successful IV measurements of the product. Calculation of glacier area is based on the RGI 5.0 (Pfeffer et al., 2014) with outlines for this region provided by Glaciers_cci. Overall 91% of the glaciers are covered by IV measurements. There are some gaps on the slower inland glaciers where there are less features and in some of the shearing zones on the faster glaciers.
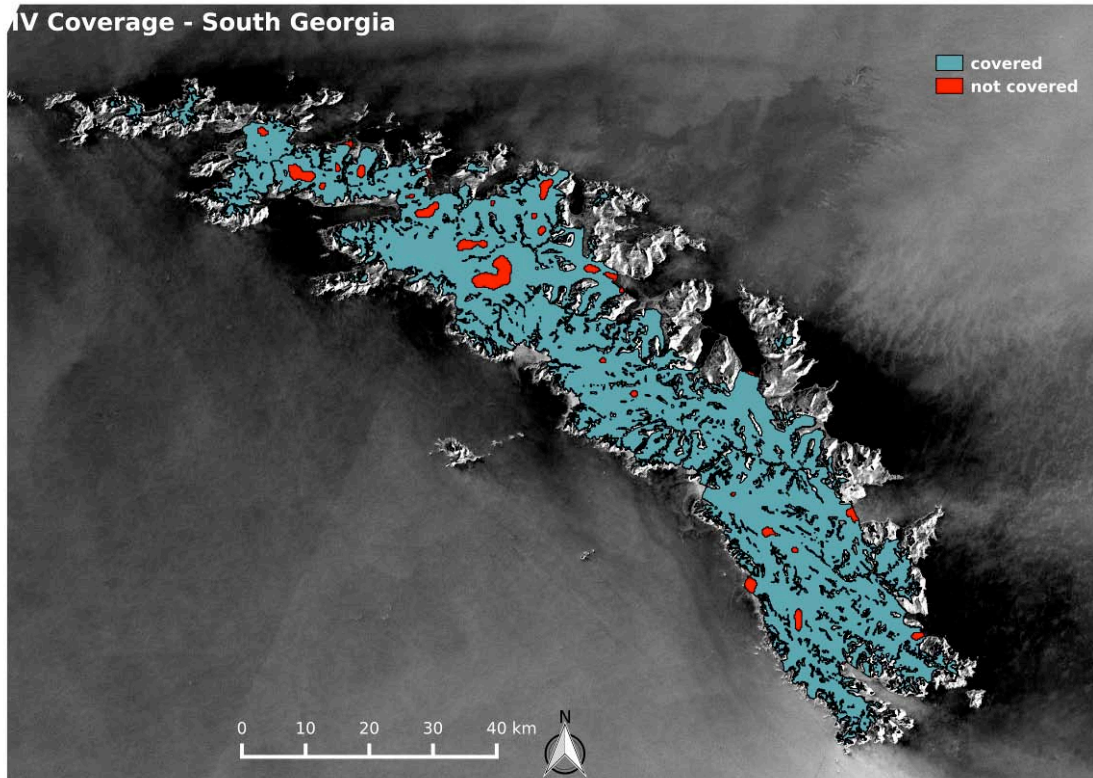
*Figure 6.22: Outline of glacierized terrain in South Georgia based on RGI 5.0 (Pfeffer et al., 2014) and indication of IV coverage (cyan: covered, red: not covered). Background: Sentinel-1 amplitude mosaic.*

| Sensor/Product ID | Glacier area [km$^2$] | IV area [km$^2$] | Coverage [%] |
|---|---|---|---|
| S-1 SAR/IV_rgi19_006 | 2,188 | 1,992 | 91.0 |

*Table 6.13: Total glacier area, IV area and percentage coverage for the Sentinel-1 IV product covering South Georgia.*

### 6.8.2.  QA-IV-3: Stable Rock analysis of IV products

The ice covered (moving) terrain is separated from ice-free (stable) terrain (see Figure 6.13). The masking is done using a polygon of glacier outlines based on RGI 5.0. Buffers around the glacier polygon are applied before extraction of stable ground for statistics calculation. The analysis has been performed for both easting and northing velocity components. The quality metrics of the test provide mean and RMSE of the velocity over stable terrain. Results show that both the northing and easting velocity components are scattered around a zero-mean indicating no bias, and with a low RMSE of 3 cm/d (Table 6.20).

| Sensor/Product ID | Number of pixels | Mean E [m d$^{-1}$] | RMSE E [m d$^{-1}$] | Mean N [m d$^{-1}$] | RMSE N [m d$^{-1}$] |
|---|---|---|---|---|---|
| PALSAR/IV_rgi19_006 | 30,249 | 0.00 | 0.03 | 0.00 | 0.03 |

*Table 6.20: Summary of stable rock quality assessment for Sentinel-1 derived velocities on South Georgia.*

**glaciers cci**

Contract: 4000109873/14/I-NB
Product Validation and Inter-comparison Report (PVIR)

Name:      Glaciers_cci-D4.1_PVIR
Version:   1.6
Date:      21.12. 2017
Page:      49

## 6.9.  Product: Ice Velocity Svalbard (ID: IV_rgi07_006)

The IV data set provides a velocity mosaic of glaciers in the Svalbard Archipelago. Ice velocity is derived by SAR offset tracking using Sentinel-1 image pairs acquired in Interferometric Wide Swath (IW) mode and is averaged over the period Jan 2015 to Jan 2017. The final product is clipped using an ocean mask based on Landsat imagery with calving fronts updated to 2014-2016. The data set is comprised of a compressed ASCII tables (csv format) as specified in the PSD listing the three velocity components (easting, northing and vertical) in metres per day (m d$^{-1}$) in UTM 33N projection as well as in (3-layer) GeoTiff format. The vertical velocity is derived from the interpolated height difference of the end position of the displacement vector and the start position, taken from the Norwegian Polar Institute Terrengmodell Svalbard (NPI, 2014). The data product is posted at 250 m and includes an xml file (metadata) and a quicklook image. Figure 6. shows the magnitude of the horizontal velocity depicted on a Sentinel-1 amplitude image. For the data set the quality tests QA-IV-2, QA-IV-3 were applied.
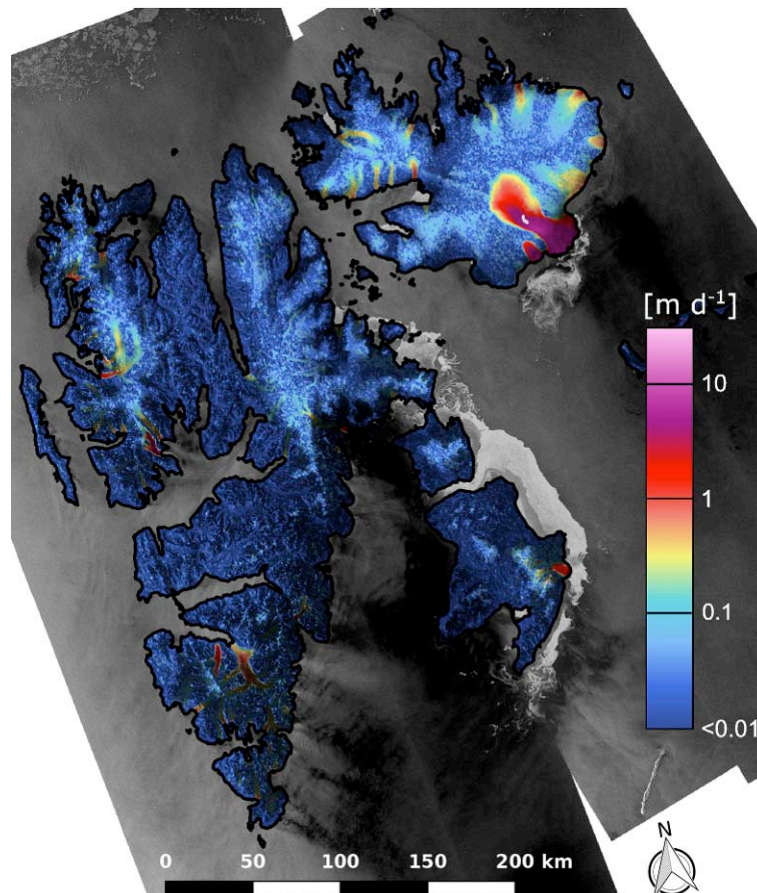


*Figure 6.23: IV map of Svalbard from Sentinel-1 data acquired from Jan 2015 to Jan 2017. Background: Sentinel-1 amplitude mosaic.*

### 6.9.1.  QA-IV-2: Coverage of IV measurements

Figure 6.2424 and Table 6.214 give an overview of the total area of Svalbard and the coverage of successful IV measurements for the product. For the outline, we use an ocean mask

based on manual delineation of Landsat imagery with calving fronts updated to 2014-2016. Overall nearly 100% of the glaciers are covered by IV measurements. There are some gaps on the slower inland glaciers where there are less features and in some of the shearing zones on the faster glaciers.
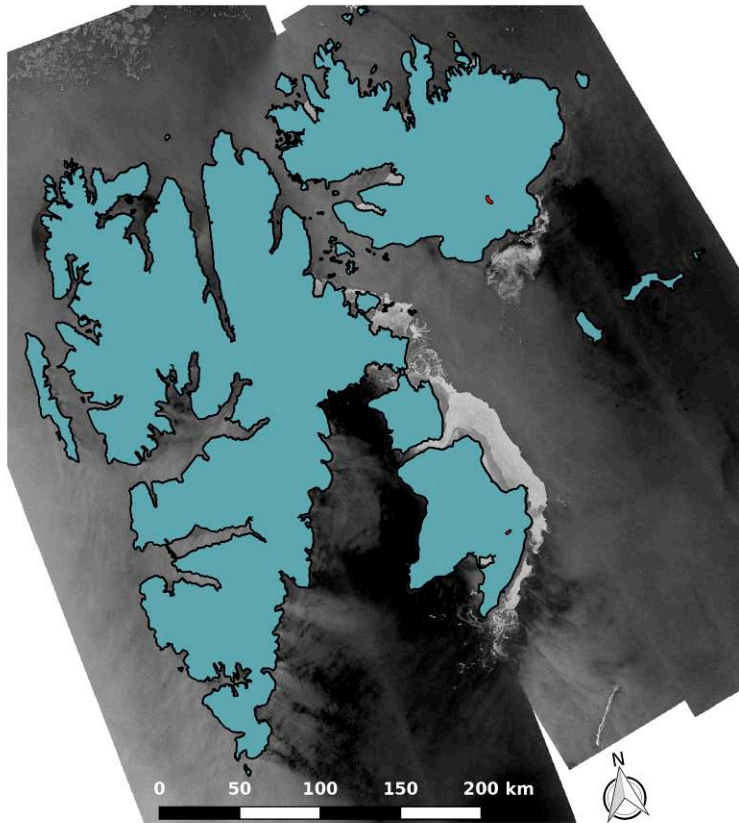


*Figure 6.24: Outline of Svalbard based on Landsat imagery with calving fronts updated to 2014-2016 and indication of IV coverage (cyan: covered, red: not covered). Background: Sentinel-1 amplitude mosaic.*

| Sensor/Product ID | Glacier area [km$^2$] | IV area [km$^2$] | Coverage [%] |
| --- | --- | --- | --- |
| S-1 SAR/IV_rgi19_006 | 60,165 | 59,430 | 99.78 |

*Table 6.214: Total glacier area, IV area and percentage coverage for the Sentinel-1 IV product covering Svalbard.*

### 6.9.2. QA-IV-3: Stable Rock analysis of IV products

The ice covered (moving) terrain is separated from ice-free (stable) terrain (Figure 6.225). The masking is done using a polygon of glacier outlines based on RGI 5.0. Buffers around the glacier polygon are applied before extraction of stable ground for statistics calculation. The analysis has been performed for both easting and northing velocity components. The quality metrics of the test provide mean and RMSE of the velocity over stable terrain. Results show that both the northing and easting velocity components are scattered around a zero-mean indicating no bias, and with a low RMSE of 2 cm/d (Table 6.22).
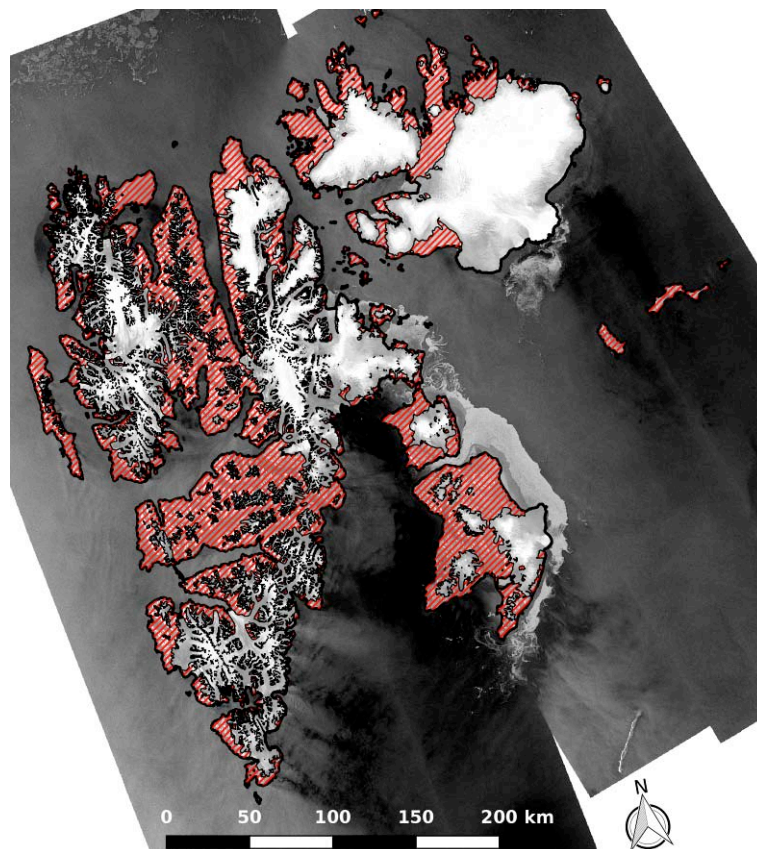


*Figure 6.25: Stable rock area in Svalbard based on RGI 5.0 (Pfeffer et al., 2014) and used for the stable rock analysis. Background: Sentinel-1 amplitude image.*

| Sensor/Product ID | Number of pixels | Mean E [m d$^{-1}$] | RMSE E [m d$^{-1}$] | Mean N [m d$^{-1}$] | RMSE N [m d$^{-1}$] |
|---|---|---|---|---|---|
| S-1 SAR/IV_rgi07_006 | 392,657 | 0.00 | 0.01 | 0.00 | 0.02 |

*Table 6.22: Summary of stable rock quality assessment for Sentinel-1 derived velocities in Svalbard.*

Contract: 4000109873/14/I-NB

Product Validation and Inter-
comparison Report (PVIR)

Name: Glaciers_cci-D4.1_PVIR
Version: 1.6
Date: 21.12. 2017
Page: 52

# 7. References

Bajracharya, S.R. and Shrestha, B. (eds.) (2011): The status of glaciers in the Hindu Kush-Himalayan region. Kathmandu: ICIMOD, 130 pp.

Flament, T. and Rémy, F. (2012): Dynamic thinning of Antarctic glaciers from along-track repeat radar altimetry. Journal of Glaciology, 58 (211), 830-840.

Glaciers_cci (2014): Climate Research Data Package - Technical Note (CRDP). Prepared by the Glaciers_cci consortium, 29 pp. (http://glaciers-cci.enveo.at/crdp2.html)

Guo, W., S. Liu, J. Xu, L. Wu, D. Shangguan, X. Yao, J. Wei, W. Bao, P. Yu, Q. Liu, Z. Jiang (2015): The second Chinese glacier inventory: data, methods and results. Journal of Glaciology, 61 (226), 357-372.

Liu, H., K. Jezek, B. Li, and Z. Zhao (2001): Radarsat Antarctic Mapping Project Digital Elevation Model, Version 2. Boulder, Colorado USA. NASA National Snow and Ice Data Center Distributed Active Archive Center.

Norwegian Polar Institute. 2014. Terrengmodell Svalbard (Terrengmodell Svalbard 20 m). Norwegian Polar Institute. (doi: 10.21334/npolar.2014.dce53a47)

Nuimura, T., A. Sakai, K. Taniguchi, H. Nagai, D. Lamsal, S. Tsutaki, A. Kozawa, Y. Hoshina, S. Takenaka, S. Omiya, K. Tsunematsu, P. Tshering, and K. Fujita (2015): The GAMDAM glacier inventory: a quality-controlled inventory of Asian glaciers. The Cryosphere, 9, 849-864.

Pfeffer, W.T., A.A. Arendt, A. Bliss, T. Bolch, J.G. Cogley, A.S. Gardner, J.O. Hagen, R. Hock, G. Kaser, C. Kienholz, E.S. Miles, G. Moholdt, N. Mölg, F. Paul, V. Radić, P. Rastner, B.H. Raup, J. Rich, M.J. Sharp and the Randolph Consortium (2014): The Randolph Glacier Inventory: a globally complete inventory of glaciers, J. Glaciol., 60 (221), 537-551.

Raup, B.H., A. Racoviteanu, S.J.S. Khalsa, C. Helm, R. Armstrong, Y. Arnaud (2007): The GLIMS Geospatial Glacier Database: a New Tool for Studying Glacier Change. Global and Planetary Change, 56,101-110.

Raup, B., and 20 others (2014): Quality in the GLIMS Glacier Database. In: Kargel, J.S., Bishop, M.P., Kääb, A. and Raup, B.H. (Eds.): Global Land Ice Measurements from Space - Satellite Multispectral Imaging of Glaciers. Praxis-Springer, Chapter 7, 163-180.

Rastner, P., T. Bolch, N. Mölg, H. Machguth, R. Le Bris and F. Paul (2012): The first complete inventory of the local glaciers and ice caps on Greenland. The Cryosphere, 6, 1483-1495.

Rastner, P., Strozzi, T. and Paul, F. (2017): Fusion of multi-source satellite data and DEMs to create a new glacier inventory for Novaya Zemlya. Remote Sensing

Rignot, E., J. Mouginot, and B. Scheuchl. 2011. Ice Flow of the Antarctic Ice Sheet. Science, 333 (6048), 1427-1430.

Smith, B.E., Fricker, H.A., Joughin, I.R. and Tulaczyk, S. (2009): An inventory of active subglacial lakes in Antarctica detected by ICESat (2003-2008). Journal of Glaciology, 55 (192), 573-595.

Schwaizer, G., Nagler, T., Wuite, J., Ripper, E., Rott, H. (2016): Exploiting the new Sentinel-2 satellite data for monitoring glacier parameters. Cryosphere-Posters CRYO-86, ESA Living Planet Symposium, Prague, 9-13 May 2016.

U.S. Geological Survey (USGS), 2015-05-11, ASTER GLOBAL Digital Elevation Model V002: Ministry of Economy, Trade and Industry (METI) of Japan and the United States National Aeronautics and Space Administration (NASA): Japan and U.S., https://lpdaac.usgs.gov/products/aster_products_table/astgtm, http://LPDAAC.usgs.gov.

# 8. Acronyms

| | |
|---|---|
| ADD | Antarctic Digital Database |
| ALOS | Advanced Land Observing Satellite |
| ASCII | American Standard Code for Information Interchange |
| ATM | Airborne Topographic Mapper |
| CC | Correlation Coefficient |
| CGI | Chinese Glacier Inventory |
| CS2 | Cryosat 2 |
| CSV | Comma Separated Value |
| DEM | Digital Elevation Model |
| DGPS | Differential Global Positioning System |
| ECA | Elevation Change Altimetry |
| ECDD | Elevation Change DEM differencing |
| ENVISAT | Environmental Satellite |
| EO | Earth Observation |
| ERS | European Remote-sensing Satellite |
| ETM+ | Enhanced Thematic Mapper plus |
| FBD | Fine Beam Dual |
| FBS | Fine Beam Single |
| FT | Fourier Transformation |
| GAMDAM | Glacier Area Mapping for Discharge from the Asian Mountains |
| GLIMS | Global Land Ice Measurements from Space |
| GO | Glacier Outline |
| GPS | Global Positioning System |
| HMA | High Mountain Asia |
| ICESat | Ice, Cloud, and land Elevation Satellite |
| ICIMOD | Internationl Centre for Integrated Mountain Development |
| ID | Identifier |
| InSAR | Interferometric SAR |
| N/A | Not Available |
| PALSAR | Phased Array type L-band Synthetic Aperture Radar |
| IV | Ice Velocity |
| QA | Quality Assessment |
| RADAR | Radio Detection and Ranging |
| RMSE | Root Mean Square Error |
| SAR | Synthetic Aperture Radar |
| SCAR | Scientific Committee on Antarctic Research |
| SNR | Signal-to-Noise Ratio |
| SPOT | System Pour l'Observation de la Terre |
| SRTM | Shuttle Radar Topography Mission |
| STD | Standard Deviation |
| TM | Thematic Mapper |
| TSX | TerraSAR-X |
| UCR | Uncertainty Characterisation Report |